

X-ray Science in the 21st Century
KITP Conference August 2 – August 6, 2010

*Probing Molecular Structure and
Electron Dynamics Using Synchrotron
Radiation, IR Laser, and FEL*

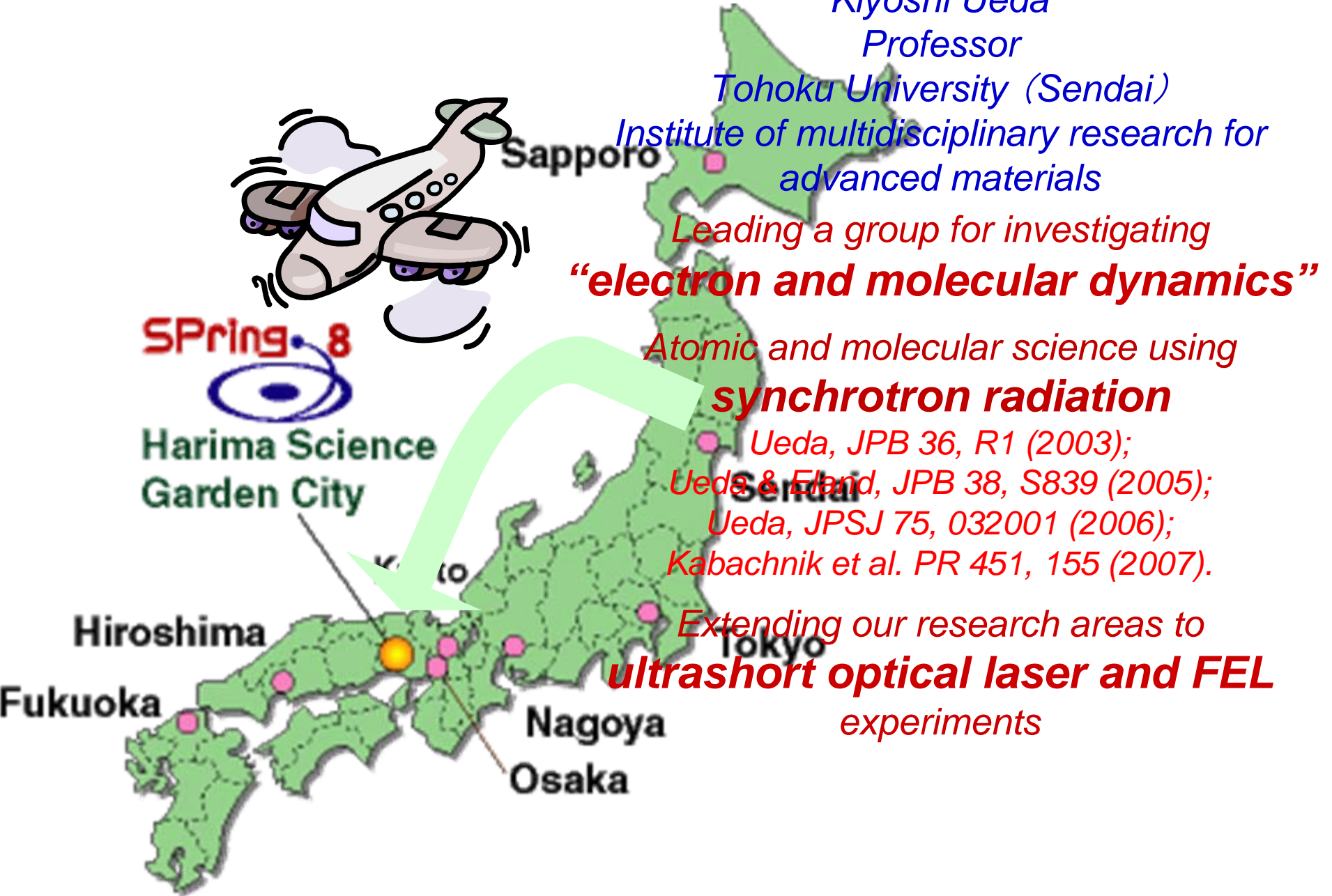
*Kiyoshi Ueda
Tohoku University, Japan*

Santa Barbara



AMO meets CDI in Santa Barbara

Introduction....



SPring-8 XFEL



Project Leader: Tetsuya Ishikawa (RIKEN)



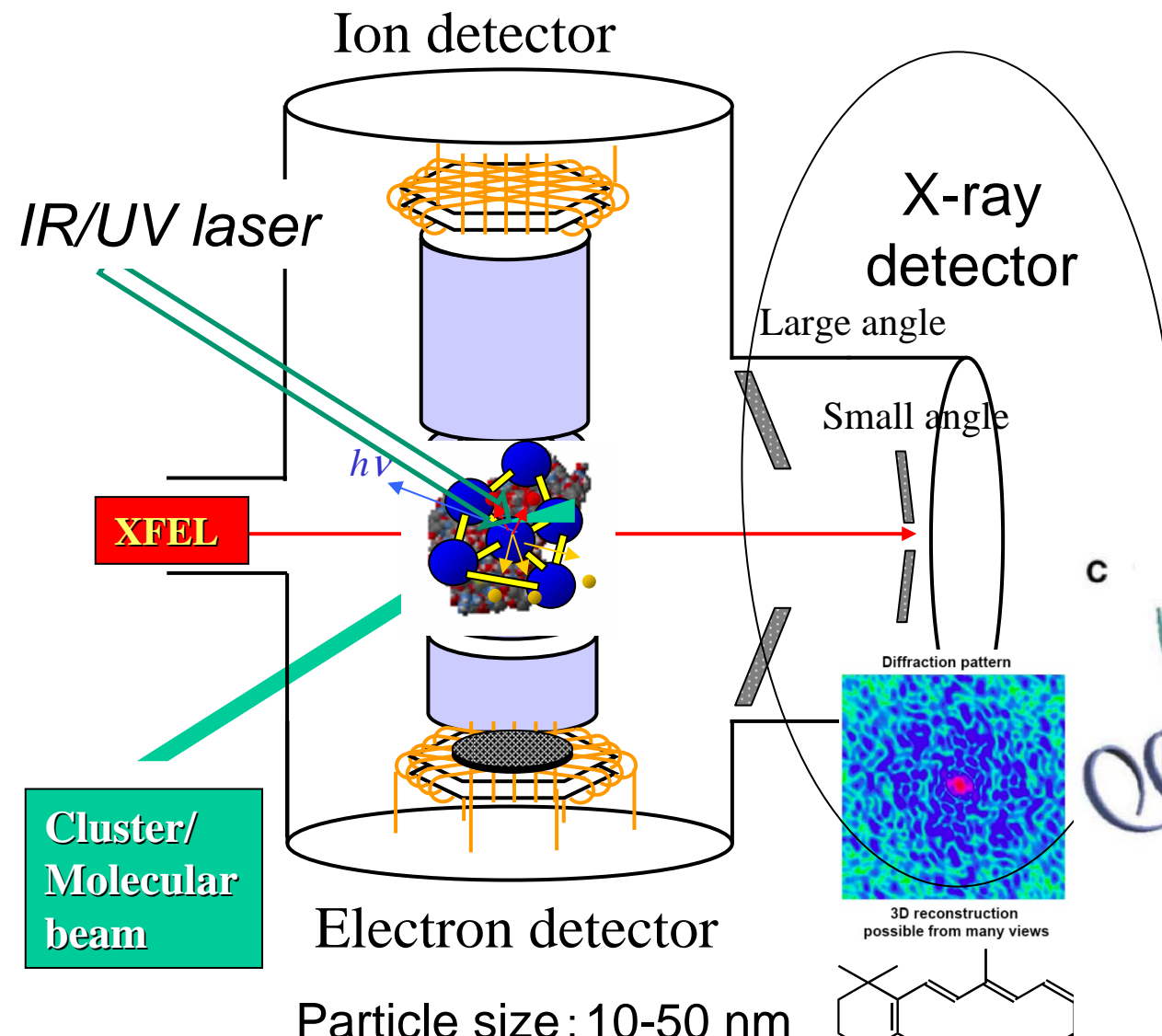
*Tetsuya Ishikawa
RIKEN*



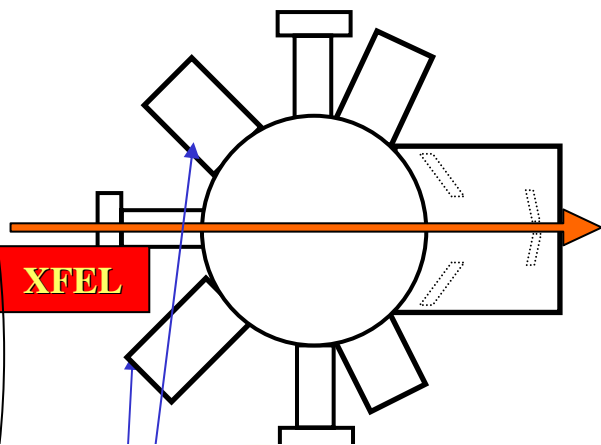
*Tsumoru Shintake
RIKEN*

Molecular Movie:

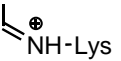
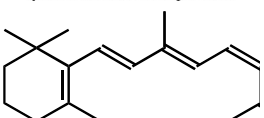
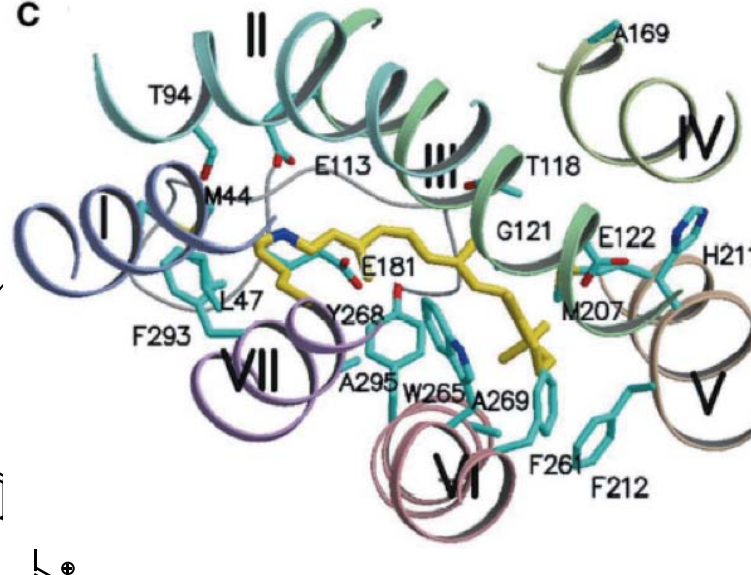
Coherent diffractive imaging of a single particle, undergoing photo-reaction, combined with coulomb explosion ion imaging and photoelectron diffraction



View from upper side



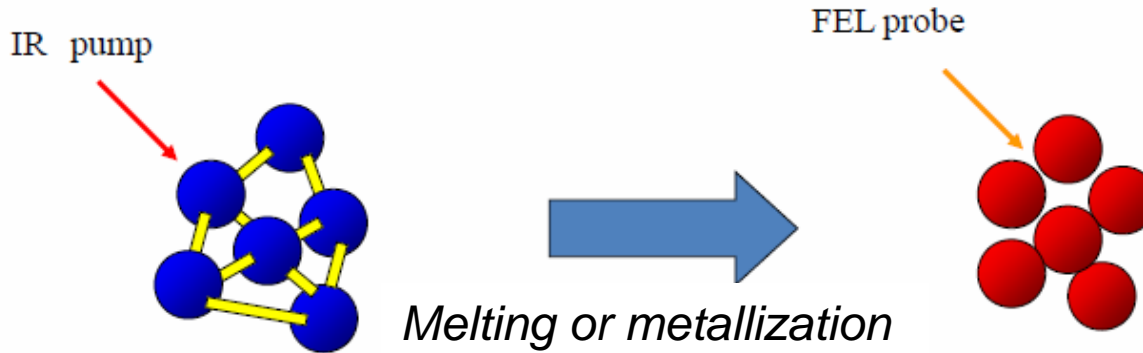
C



Particle size: 10-50 nm

Phase transition in nano-crystals or nano-clusters

A single nano-cluster or nano-crystal will be “pumped” by IR laser to “heat” them up. Melting or metallization may occur. The atomic displacement will be investigated by x-ray diffraction as a function of time delay of the x-ray pulse.



Conformation change of photo-reactive bio-molecules

A single photo-sensitive giant bio-molecule will be "pumped" by UV laser to trigger photoreaction and time-resolved coherent diffraction image will be recorded. Here, post analysis of simultaneous recording of Coulomb explosion ion momentum spectroscopy may help defining the molecular orientation.

For relatively small bio-molecules, x-ray diffraction may not work because the signals may be embedded in the background. In such a case, **x-ray core-level photoelectron diffraction** using X-FEL would be an alternative approach to extract the structure evolving in time.

Outline

I. From molecular imaging to molecular movies

1. **Introduction to molecular movie**

Time-resolved coherent X-ray diffraction imaging of a single particle, undergoing photoreaction, together with multi-particle momentum imaging

2. **Current status of molecular imaging**

- A. Laser-induced rescattering photoelectron spectroscopy
- B. Core-level photoelectron diffraction using synchrotron radiation

II. Probing electron dynamics, catching electron motion

1. **Introduction to catching electron motion**

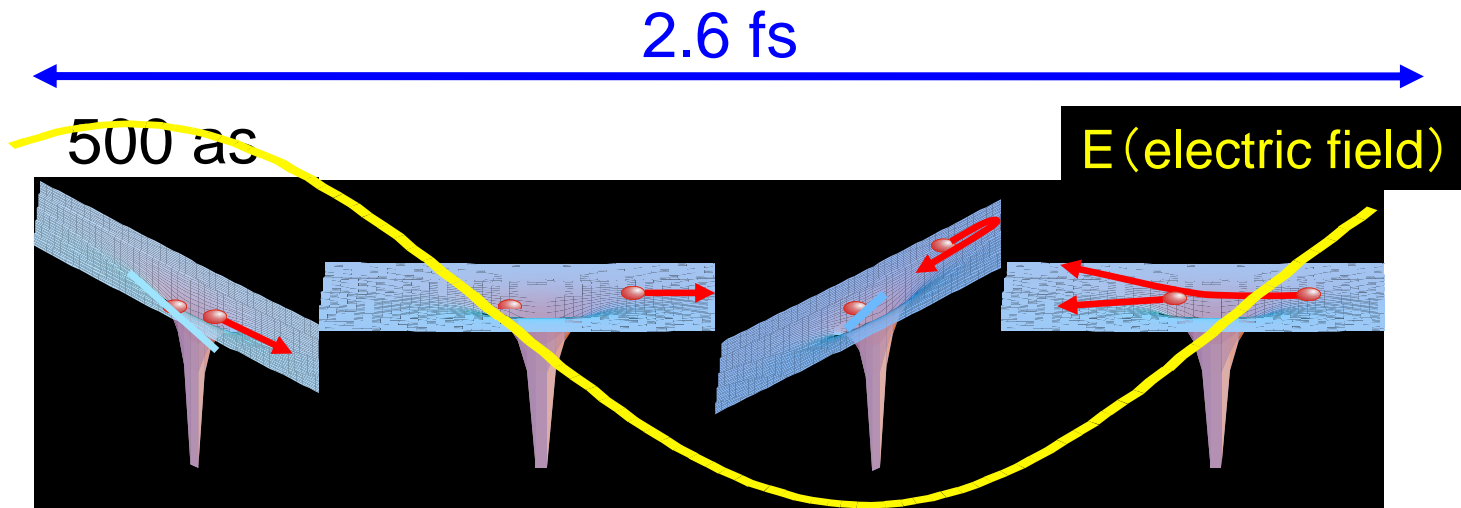
Attosecond X-ray pump-probe spectroscopy for probing charge migration

2. **Current status of electron dynamics study in energy domain**

- A. Interatomic Coulombic decay in rare-gas dimers
- B. Charge migration in clusters

Rescattering Photoelectron Spectroscopy

An electron produced by the tunnel ionization may re-collide with the parent ion. Then, spectra of the “rescattering photoelectron” provide the information about the target structure, because this rescattering process is equivalent to the elastic scattering of the free electron by the ion, at the electron momentum at the time of rescattering.



Tunnel ionization

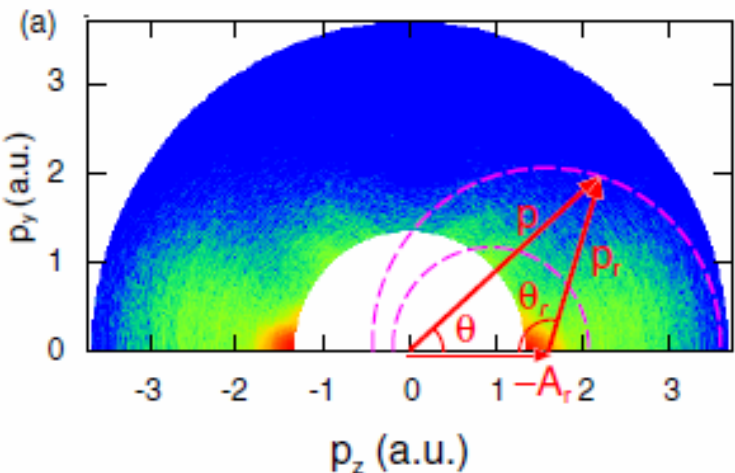
Propagation

Return

Rescattering

resolution: sub fs, sub Å (@ 800 nm)

Extraction of differential electron–ion elastic scattering cross sections from rescattering photoelectron spectra of rare gas atoms



$$D(\mathbf{p}) = W(p_r)\sigma(p_r, \theta_r),$$

$$p_z = p \cos \theta = \pm(p_r/1.26 - p_r \cos \theta_r),$$

$$p_y = p \sin \theta = p_r \sin \theta_r,$$

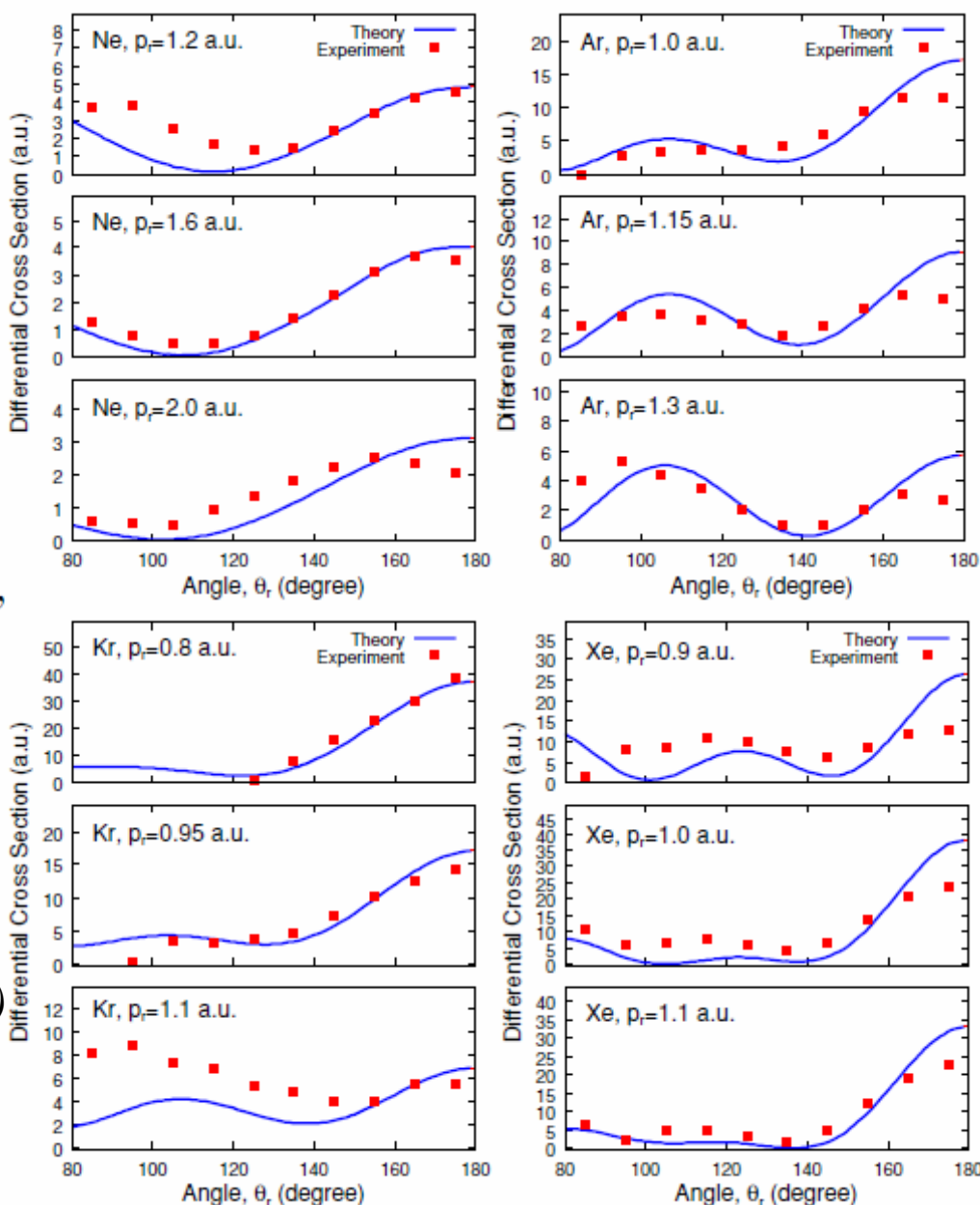
$$4Up ? < E < 10Up$$

Lower E depends on samples....

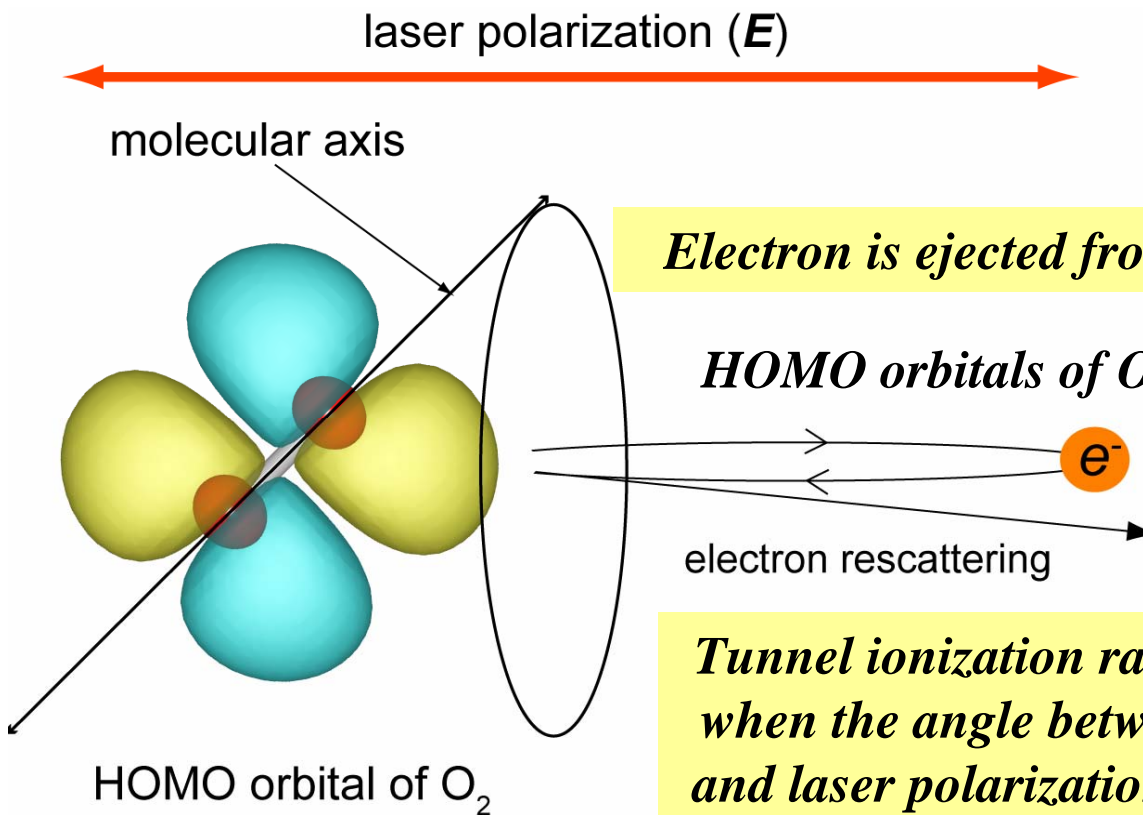
Okunishi et al., PRL 100, 143001 (2008)

Morishita et al. J. Phys. B 42, 105205 (2009)

One can retrieve a potential of the atomic ion!



Photoelectron rescattering for partially aligned O₂ and CO₂ molecules



Tunnel ionization rate is strongly enhanced when the angle between the molecular axis and laser polarization is around 45 degrees.



Measurements for partially aligned O₂ and CO₂ molecule

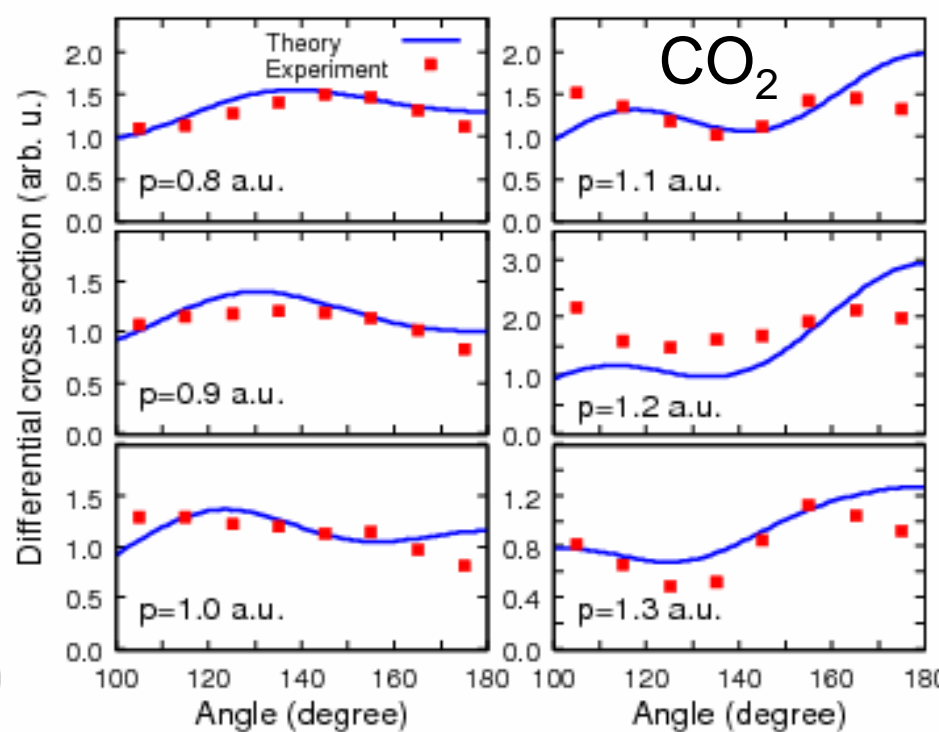
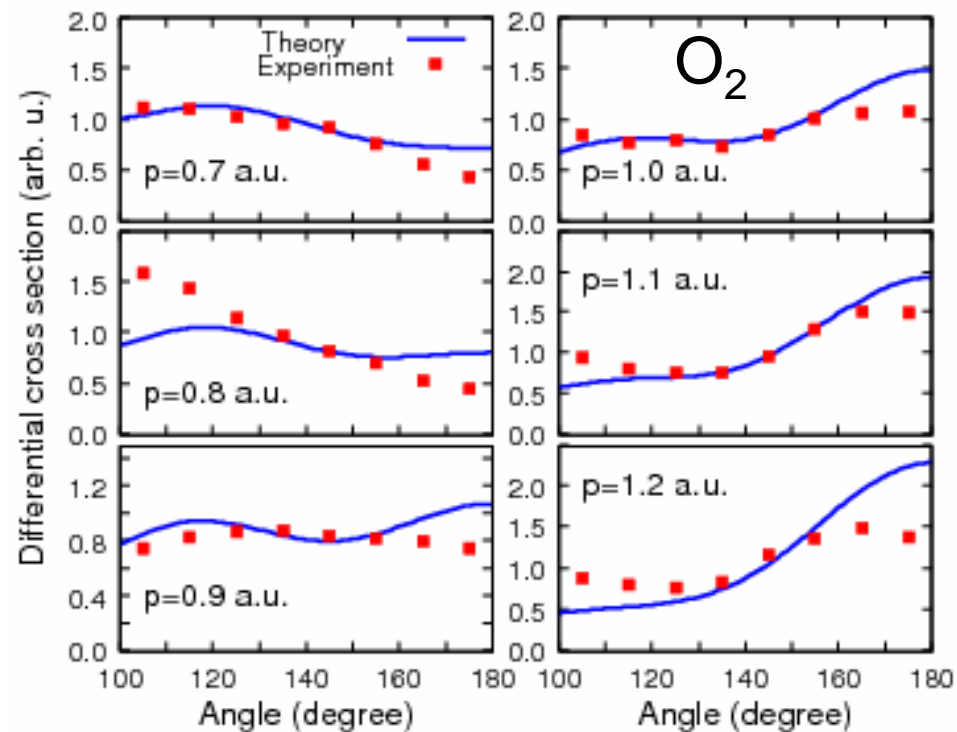
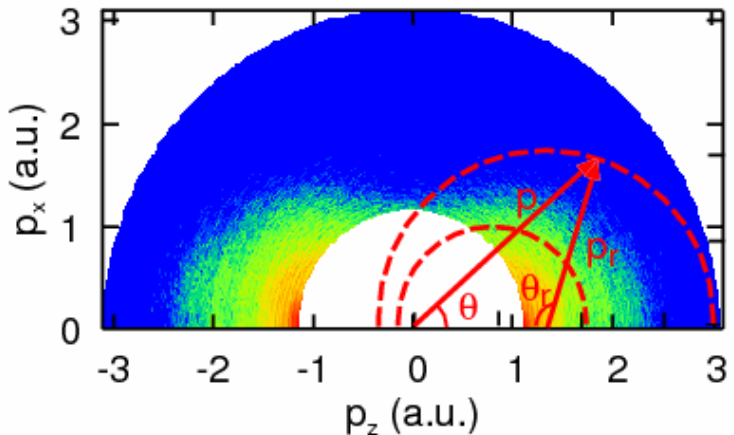
Differential cross sections (DCS) of electron–ion elastic scattering: Comparison between ab initio DCS and DCS extracted from photoelectron rescattering spectra

$$D(\mathbf{p}) = W(p_r)\sigma(p_r, \theta_r),$$

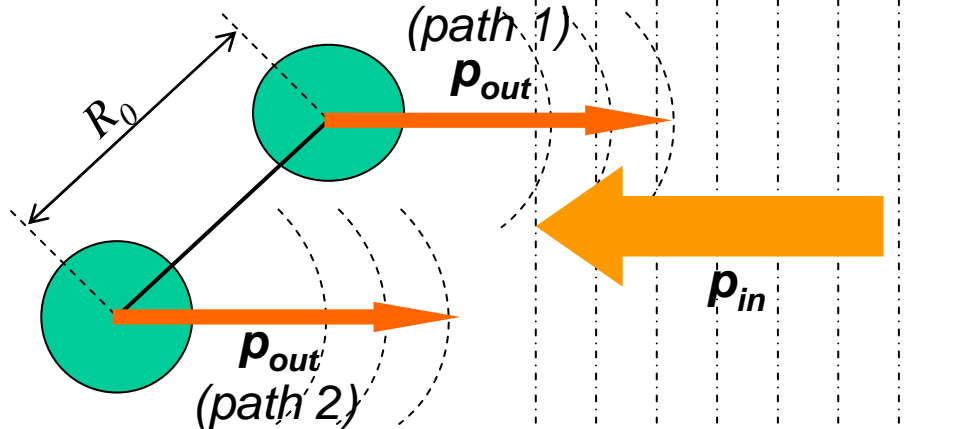
$$p_z = p \cos \theta = \pm(p_r/1.26 - p_r \cos \theta_r),$$

$$p_y = p \sin \theta = p_r \sin \theta_r,$$

Partial alignment effects of molecules are taken into account in theory using angular dependent molecular ADK ionization rates.



Simple estimation of the momentum of backward rescattered electrons



**simple plane wave
approximation**

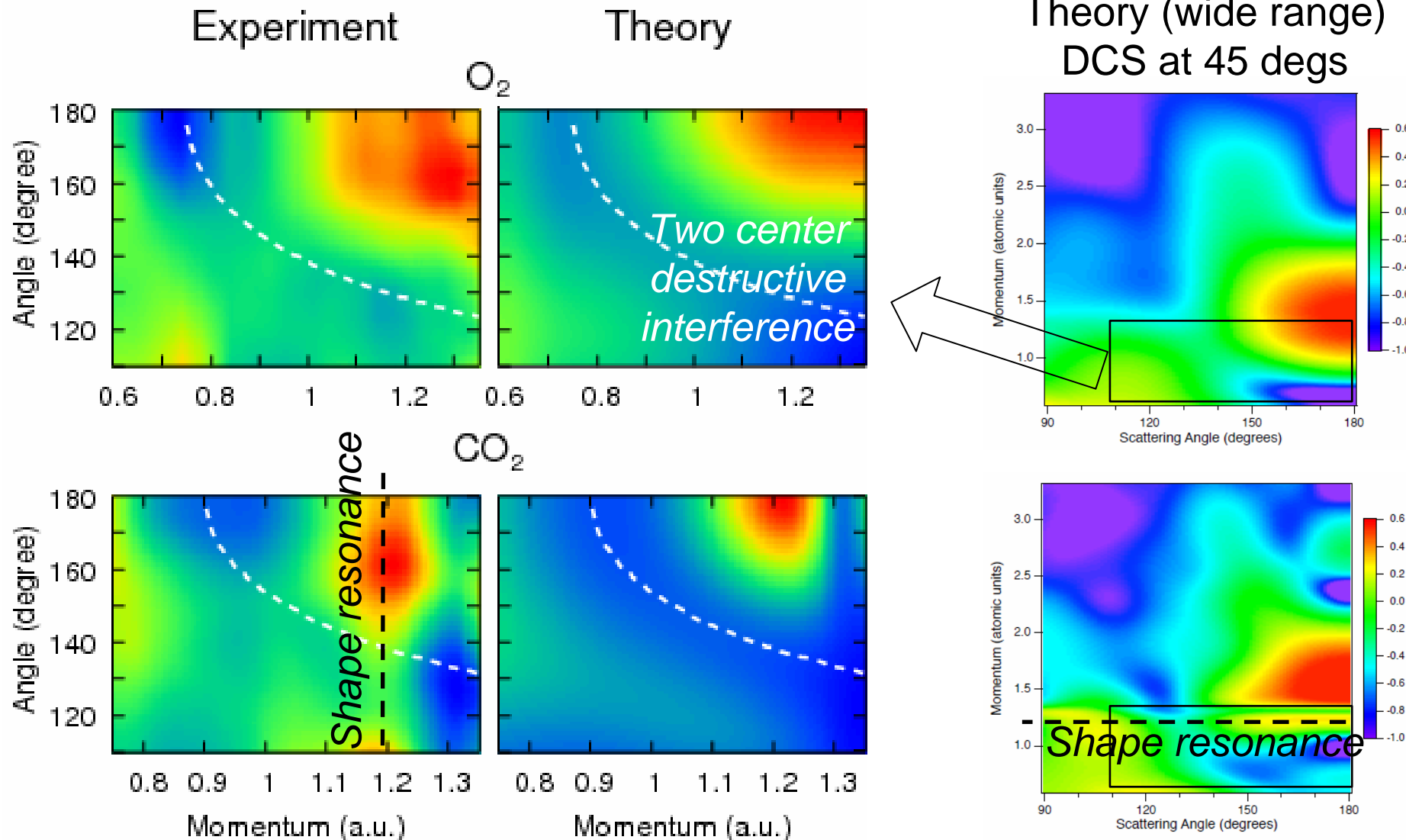
Elastic scattering
 $|\mathbf{p}_{in}| = |\mathbf{p}_{out}| = p$

difference of the path between 1 and 2 = $2 \times R_0 / \sqrt{2} = \sqrt{2}R_0$

destructive interference : $\sqrt{2}R_0 \times p = (2n+1)\pi$ (n : integer)

for O_2 $R_0=2.28$ (a.u.) $\rightarrow p= 0.97, 2.91, 4.85, \dots$ (a.u)

How to correlate DCSs with structure information



Both destructive interference and shape resonance include structure information but the plane wave approximation does not work.

Rescattering photoelectron spectroscopy collaborations

Experimental retrieval of target structure information from laser-induced rescattered photoelectron momentum distributions

M. Okunishi, T. Morishita, G. Prümper, K. Shimada, C. D. Lin, S. Watanabe, and K. Ueda
Phys. Rev. Lett. 100, 143001 (2008).

Retrieval of experimental differential electron–ion elastic scattering cross sections from high-energy ATI spectra of rare gas atoms by infrared lasers

T. Morishita, M. Okunishi, K. Shimada, G. Prümper, Z. Chen, S. Watanabe, K. Ueda, and C. D. Lin

J. Phys. B: At. Mol. Opt. Phys. 42, 105205 (6pp) (2009).

Two-Source Double-Slit Interference in Angle-Resolved High-Energy Above-Threshold Ionization Spectra of Diatoms

M. Okunishi, R. Itaya, K. Shimada, G. Prümper, K. Ueda, M. Busuladžić, A. Gazibegović-Busuladžić, D. B. Milošević, and W. Becker

Phys. Rev. Lett. 103, 043001 (2009).

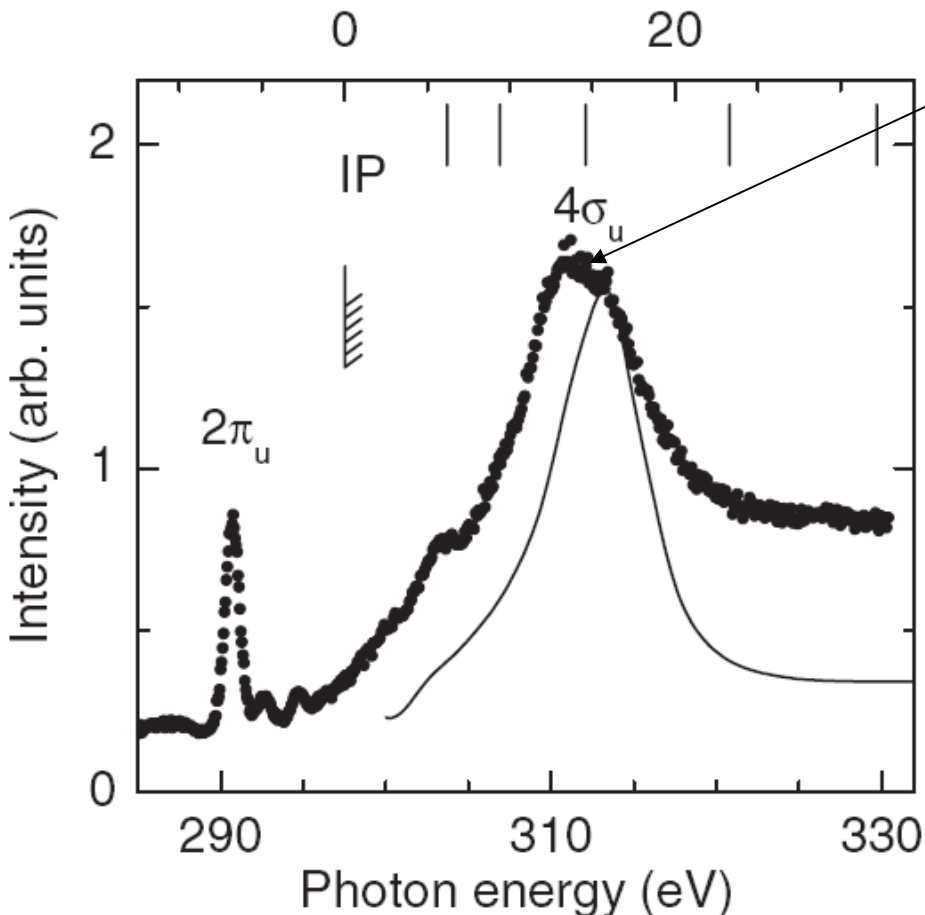
Extracting Electron-Ion Differential Cross Sections of Fixed-in-Space Molecules by Laser-induced Rescattering Photoelectron Spectroscopy

R.R. Lucchese, M. Okunishi, T. Morishita, and K. Ueda, submitted

Core-level photoelectron diffraction for fixed-in-space molecules or Molecular Frame Photoelectron Angular Distribution (MFPAD)

Total electron yield spectrum of CO₂ in the C1s ionization region

Photoelectron energy (eV)



$4\sigma_u \leftarrow 2\sigma_g$ shape resonance

CO₂ ground state configuration:

$1\sigma_g^2 1\sigma_u^2 2\sigma_g^2 3\sigma_g^2 2\sigma_u^2 4\sigma_g^2$
 $\underbrace{1\sigma_g^2}_{O1s} \underbrace{1\sigma_u^2}_{C1s} \underbrace{2\sigma_g^2}_{O2s} \underbrace{2\sigma_u^2}_{C2s} \underbrace{4\sigma_g^2}_{}$

$3\sigma_u^2 1\pi_u^4 1\pi_g^4 ({}^1\Sigma_g^+); 2\pi_u^0 5\sigma_g^0 4\sigma_u^0$

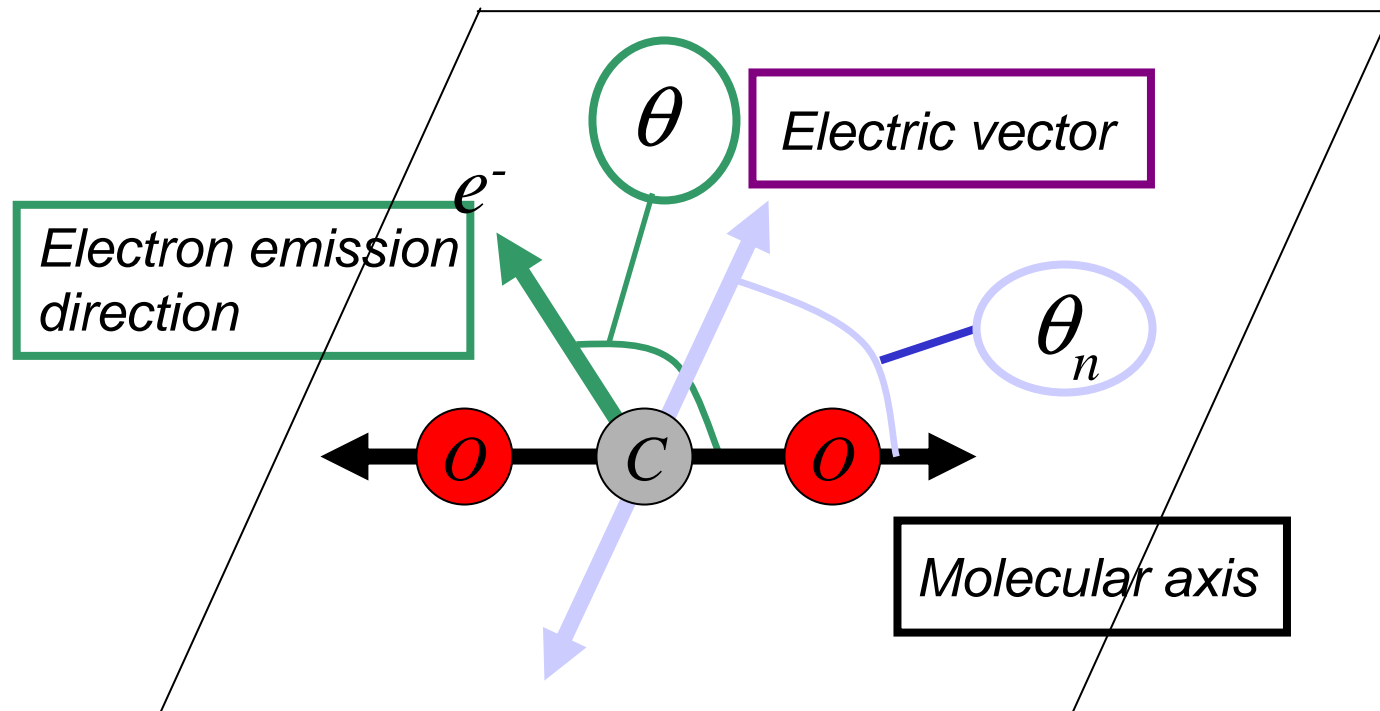
C 1s threshold
297.63 eV

N. Saito *et al.*, J. Phys. B, **36** L25 (2003).

J. D. Bozek *et al.*, Phys. Rev. A 51, 4563 (1995).

Reaction plane

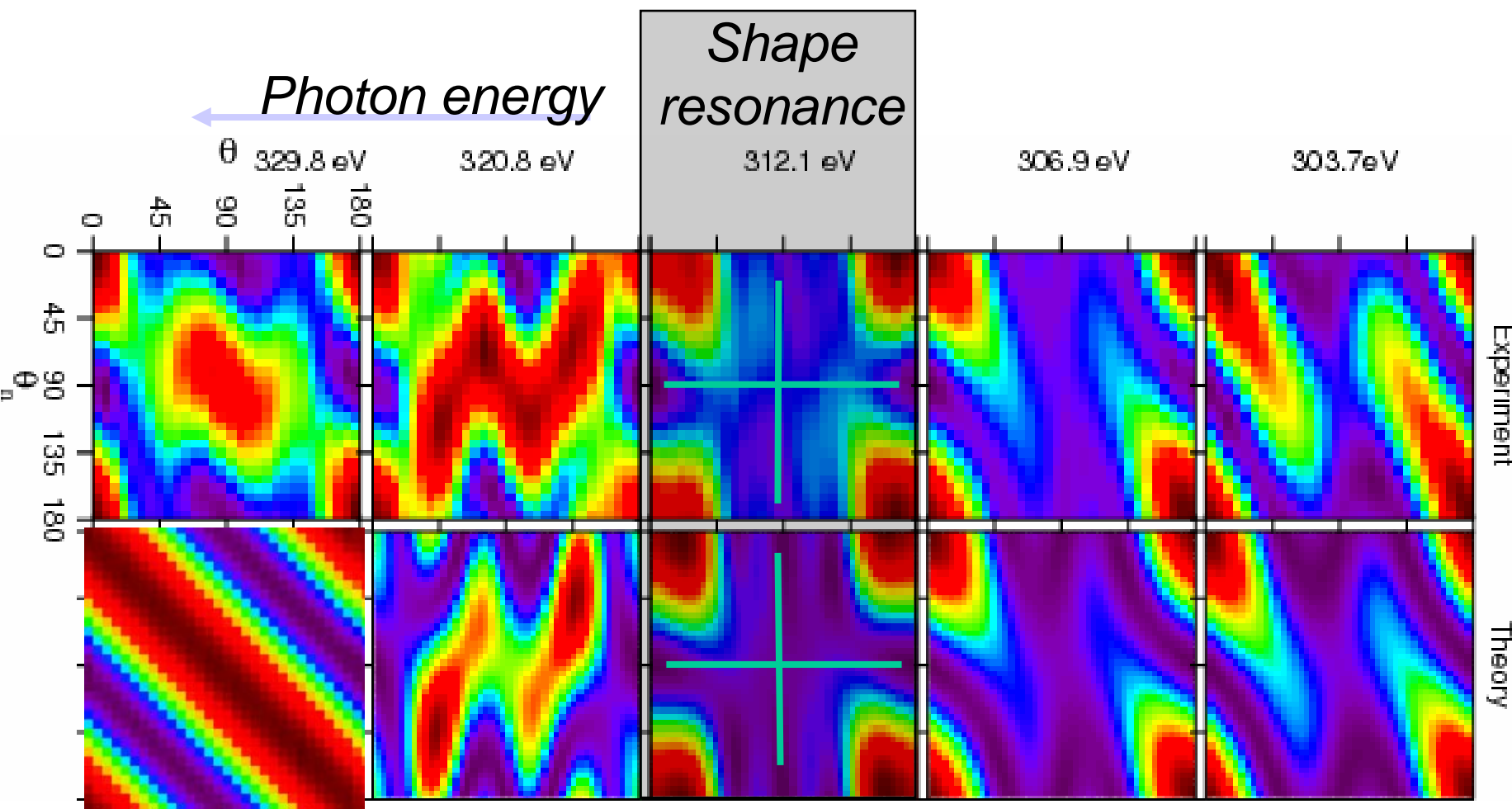
Reaction plane =plane defined by the E vector and molecular axis



We focus on the electron emission within this reaction plane

The molecular axis is defined by the O^+-CO^+ coincidence

C1s photoelectron diffraction (MFPAD) of CO₂: comparison between experiment and theory



The general agreement between experiment and theory is reasonable. At the shape resonance, the intensity drops at $\theta_n=90^\circ$ i.e. $\Sigma-\Sigma$ parallel transition. The intensity drops at $\theta=90^\circ$, i.e., σ_u photoelectron wave !

MFPAD collaborations

Carbon K-shell photoelectron angular distribution from fixed-in-space CO₂ molecules

N. Saito, A. De Fanis, K. Kubozuka, M. Machida, M. Takahashi, H. Yoshida, I.H. Suzuki, A. Cassimi, A. Czasch, L. Schmidt, **R. Dörner**, K. Wang, B. Zimmermann, **V. McKoy**, I. Koyano, and K. Ueda
J. Phys. B: At. Mol. Opt. Phys. **36**, L25 (2003).

Molecular frame photoelectron angular distribution for oxygen 1s photoemission from CO₂ molecules

N. Saito, K. Ueda, A. De Fanis, K. Kubozuka, M. Machida, I. Koyano, R. Doerner, A. Czasch, L. Schmidt, A. Cassimi, K. Wang, B. Zimmermann, and **V. McKoy**; *J. Phys. B: At. Mol. Opt. Phys.* **38**, L277-L284 (2005).

Projection methods for the analysis of MFPAD I: Minimal parameterizations in the dipole limit,

R. R. Lucchese, R. Montuoro, A. N. Grum-Grzhimailo, X.-J. Liu, G. Prümper, Y. Morishita, N. Saito, and K. Ueda,
J. Electr. Spectrosc. Relat. Phenom. **155**, 95-99 (2007)

Projection methods for the analysis of MFPADs II. Nondipole contributions

A. N. Grum-Grzhimailo, R. R. Lucchese, X.-J. Liu, G. Prümper, Y. Morishita, N. Saito, and K. Ueda,
J. Electr. Spectrosc. Relat. Phenom. **155**, 100-103 (2007)

Internal inelastic scattering satellite probed by molecular-frame photoelectron angular distributions from CO₂

X.-J. Liu, **H. Fukuzawa**, T. Teranishi, A. De Fanis, M. Takahashi, H. Yoshida, A. Cassimi, A. Czasch, L. Schmidt, R. Dörner, I. Koyano, N. Saito, and K. Ueda; **Phys. Rev. Lett.** **101**, 023001 (2008).

Breakdown of the two-step model in K-shell photoemission and subsequent decay probed by the molecular-frame photoelectron angular distributions of CO₂

X.-J. Liu, **H. Fukuzawa**, T. Teranishi, A. De Fanis, M. Takahashi, H. Yoshida, A. Cassimi, A. Czasch, L. Schmidt, R. Dörner, K. Wang, B. Zimmermann, V. McKoy, I. Koyano, N. Saito, and K. Ueda; **Phys. Rev. Lett.** **101**, 109901 (2008).

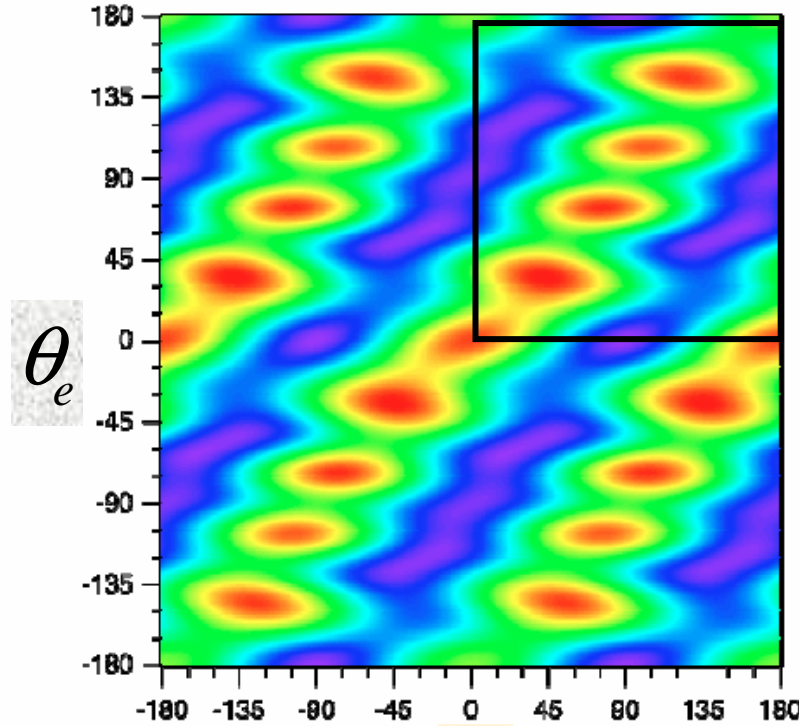
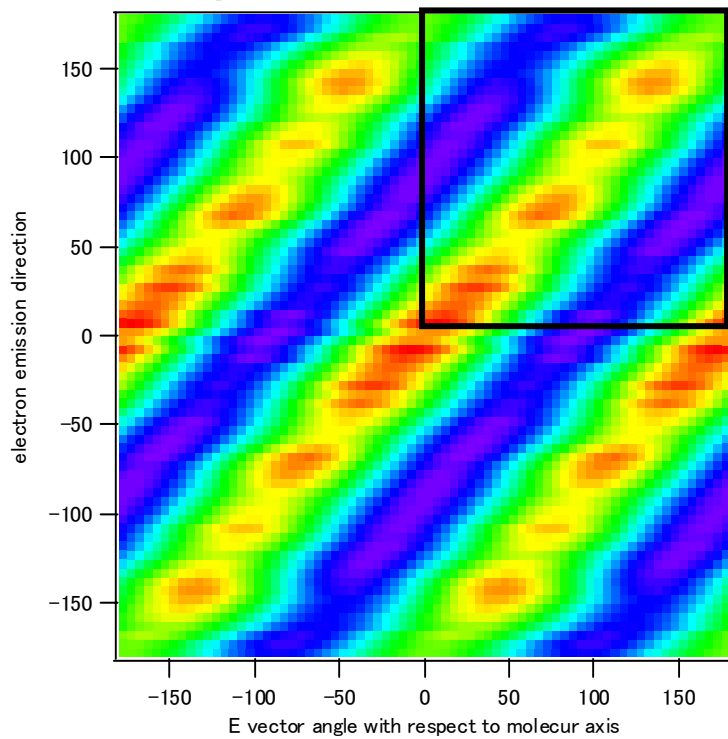
Theoretical study of asymmetric PADs for C 1s photoejection from CO₂

S. Miyabe, C.W. McCurdy, A.E. Orel, and T.N. Rescigno; *Phys. Rev. A* **79**, 053401 (2009).

Photo- and Auger Electron Angular Distributions of Fixed-in-Space CO₂

F.P. Sturm, M. Schoeffler S. Lee, T. Osipov, N. Neumann, H.-K. Kim, S. Kirschner, B. Rudek, J.B. Williams, J.D. Daughhetee, C.L. Cocke, **K. Ueda**, A.L. Landers, Th. Weber, M.H. Prior, A. Belkacem, **and R. Doerner**
Phys. Rev. A **79**, 053401 (2009).

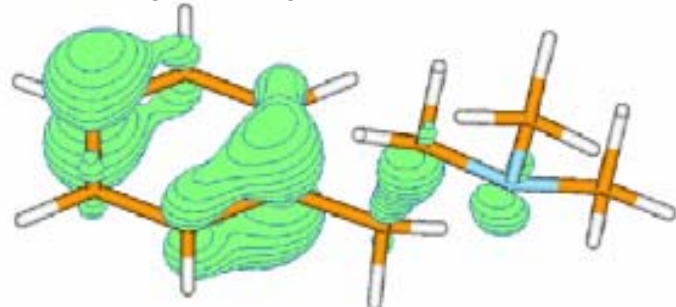
O_{1s} photoelectron diffraction (MFPAD) of CO₂: comparison between experiment and theory (574 eV)



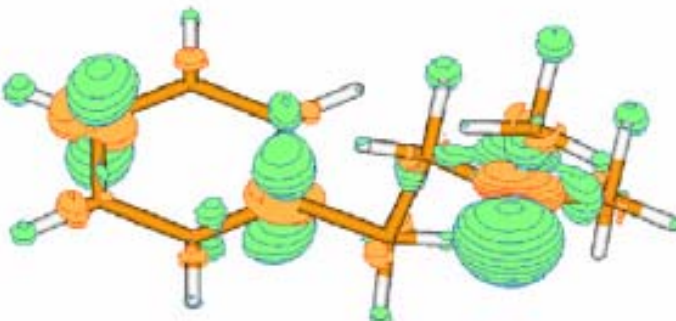
Photoelectron diffraction spectrum includes information about molecular structure. Ab initio calculations well agree with measurements. However, retrieval of the structure information based on the plane wave approximation does not work. **We need to solve the inverse problem!**

Probing electron dynamics, catching electron motion

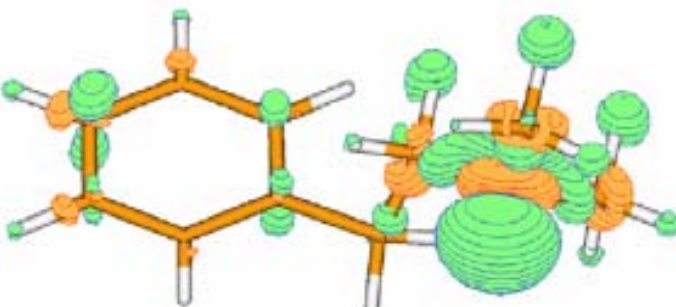
*Ultrafast charge migration in
2-phenylethyl-N,N-dimethylamine*



$t = 0$



$t = 2 \text{ fs}$



$t = 4 \text{ fs}$



Can you measure it?



Yes, we can!

*For that, we need atto-
second pulses*

Catching Electrons with Light

Julien Bertrand

Paul.Corkum@nrc.ca

Sarah Golin



VUVX Public lecture (Vancouver)

Atto-researchers (2010)



Canada
China
Cuba
England
Germany
Iran
Israel
Italy
Japan *Korea
Switzerland



* K. Ueda - an honorary member of the Atto-group



uOttawa

Need Ultra-short X-ray Pulses? Try Aluminum Foil

SLAC Today, July 27, 2010

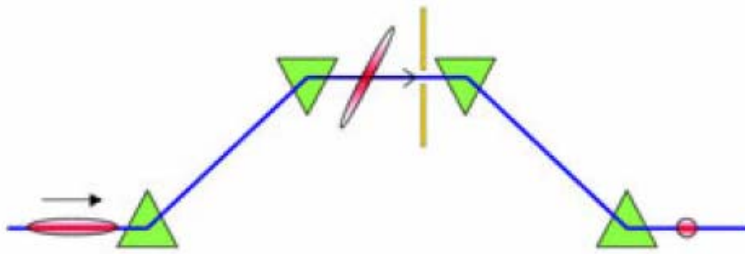
VOLUME 92, NUMBER 7

PHYSICAL REVIEW LETTERS

week ending
20 FEBRUARY 2004

Femtosecond and Subfemtosecond X-Ray Pulses from a Self-Amplified Spontaneous-Emission-Based Free-Electron Laser

P. Emma,* K. Bane, M. Cornacchia, Z. Huang, H. Schlarb,[†] G. Stupakov, and D. Walz
Stanford Linear Accelerator Center, 2575 Sand Hill Road, Menlo Park, California 94025, USA



The foil (yellow) slices each electron bunch (pink) while it is diverted into an upright shape inside a bunch compressor. The green triangles represent magnets that redirect the electrons' path of travel. (Image courtesy Paul Emma.)

But it wasn't until last week that the idea was tested experimentally. A group of SLAC physicists, including Clive Field, Mark Petree and David Kharakh, built and installed a prototype foil in early June; user experiments led by Reinhard Kienberger from the Technische Universitaet Munich, together with data collected previously by LCLS staff scientists, could determine whether the foil is, in fact, producing one-femtosecond X-ray pulses.

Attosecond X-ray pump-probe is no more a dream!

Can we catch the electron motion? Yes, we can!



Slotted foil: The open "V" (bottom) allows one bunch of electrons through; the double-slot "V"s (middle and top) create two narrow bunches. The width of the V determines the bunch width (single bunch) or timing between bunches (double-slot). (Image courtesy Paul Emma.)

Outline

I. From molecular imaging to molecular movies

1. **Introduction to molecular movie**

Time-resolved coherent X-ray diffraction imaging of a single particle, undergoing photoreaction, together with multi-particle momentum imaging

2. **Current status of molecular imaging**

- A. Core-level photoelectron diffraction
- B. Laser-induced rescattering photoelectron spectroscopy

II. Probing electron dynamics, catching electron motion

1. **Introduction to catching electron motion**

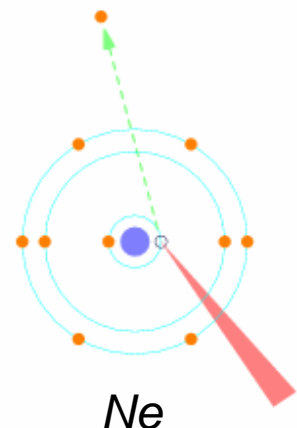
Attosecond X-ray pump-probe spectroscopy on charge migration

2. **Current status of charge migration study in energy domain**

- A. Interatomic Coulombic decay in rare-gas dimers
- B. Charge migration in clusters

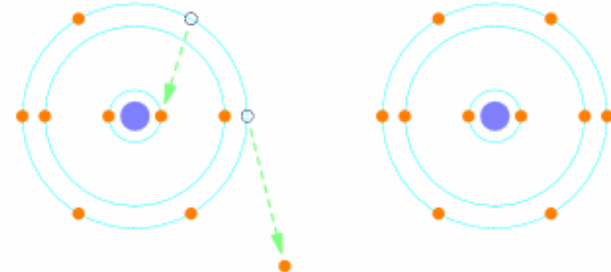
Auger vs Interatomic Coulombic Decay (ICD)

(a) Core ionization

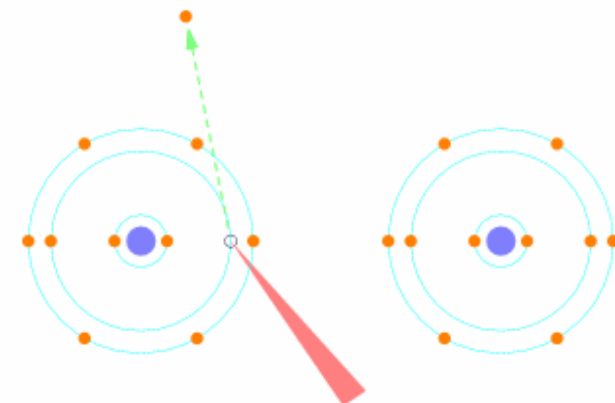


(b) Auger decay: One site state

Intra-atomic

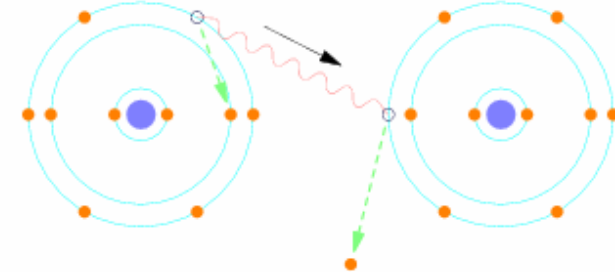


(a) Inner-valence ionization



(b) ICD decay: two site state

Inter-atomic



*ICD rate depends on
inter nuclear distance!*

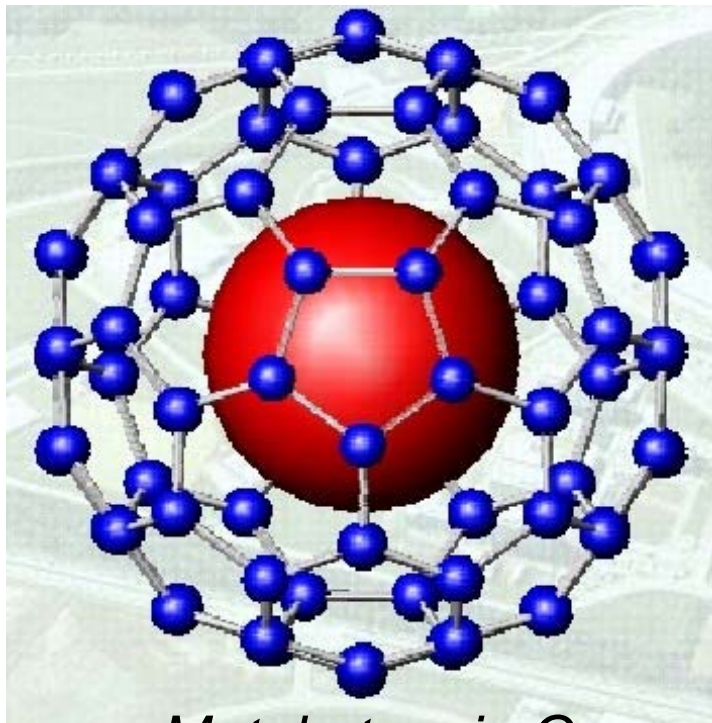
Why is ICD important?

ICD: electronic decay where the environment plays a role!

ICD occurs in van der Waals clusters, in hydrogen bonding clusters, in metallofullerenes, in bio-molecules in the living cell, etc

ICD is everywhere!

ICD is one of the key players in energy and charge transfer in these systems.



Benchmark study on Interatomic Coulombic Decay

Theoretical

First prediction - HF clusters:

L.S. Cederbaum, J. Zobeley, and F. Tarantelli, *Phys. Rev. Lett.* **79**, 4778 (1997).

Prediction - Ne dimer (and Ne clusters):

R. Santra, J. Zobeley, L.S. Cederbaum et al., *Phys. Rev. Lett.* **85**, 4490 (2000).

Experimental

First observation - Ne cluster:

U. Hergenhahn and coworkers, *Phys. Rev. Lett.* **90**, 203401 (2003).

Ne₂ e-ion-ion coincidence:

R. Dörner and coworkers, *Phys. Rev. Lett.* **93**, 163401 (2004).

Interatomic Coulombic Decay after Auger decay

Prediction - ICD from Auger final states in Ne dimer

R. Santra and L.S. Cederbaum, Phys. Rev. Lett. **90**, 153401 (2003).

Why is ICD after Auger decay important?

It may be relevant to radiation damage in bio-molecules in the living cell

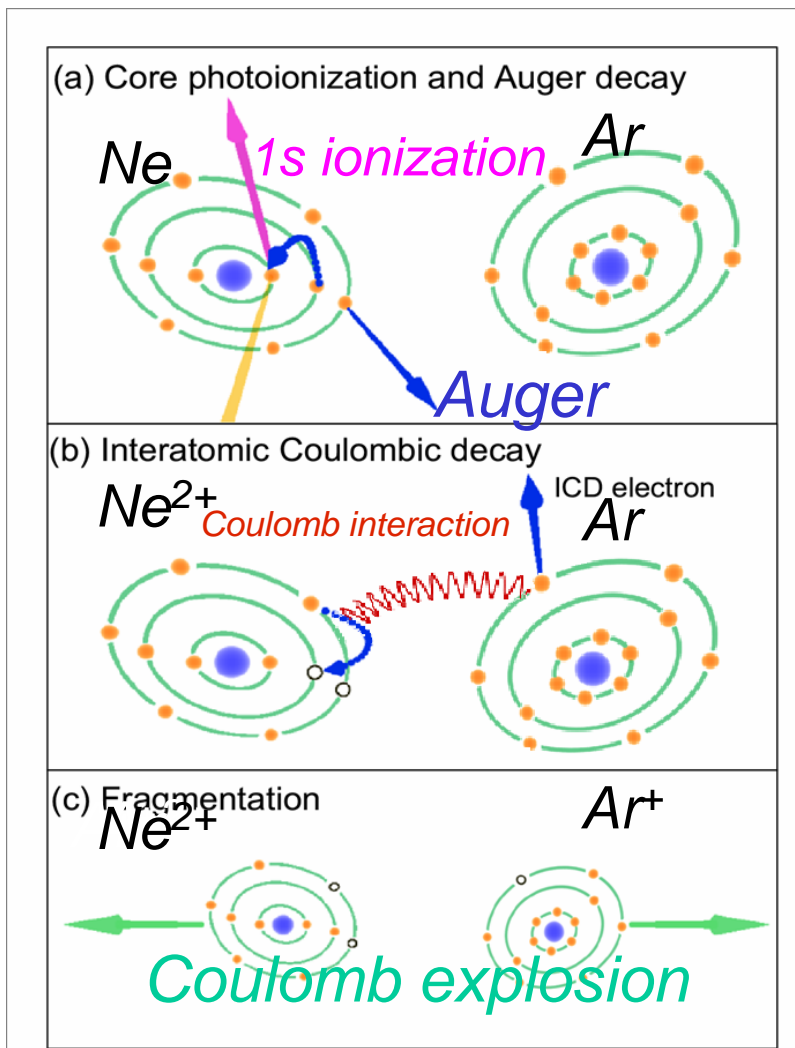
Core ionization by X-ray radiation is first step of radiation damage.

Radiation damage is known to be caused by low energy electron collisions, not high energy Auger electrons.

ICD is one of the important mechanisms to produce low energy electrons after Auger decay.

So ICD may be relevant to radiation damage!

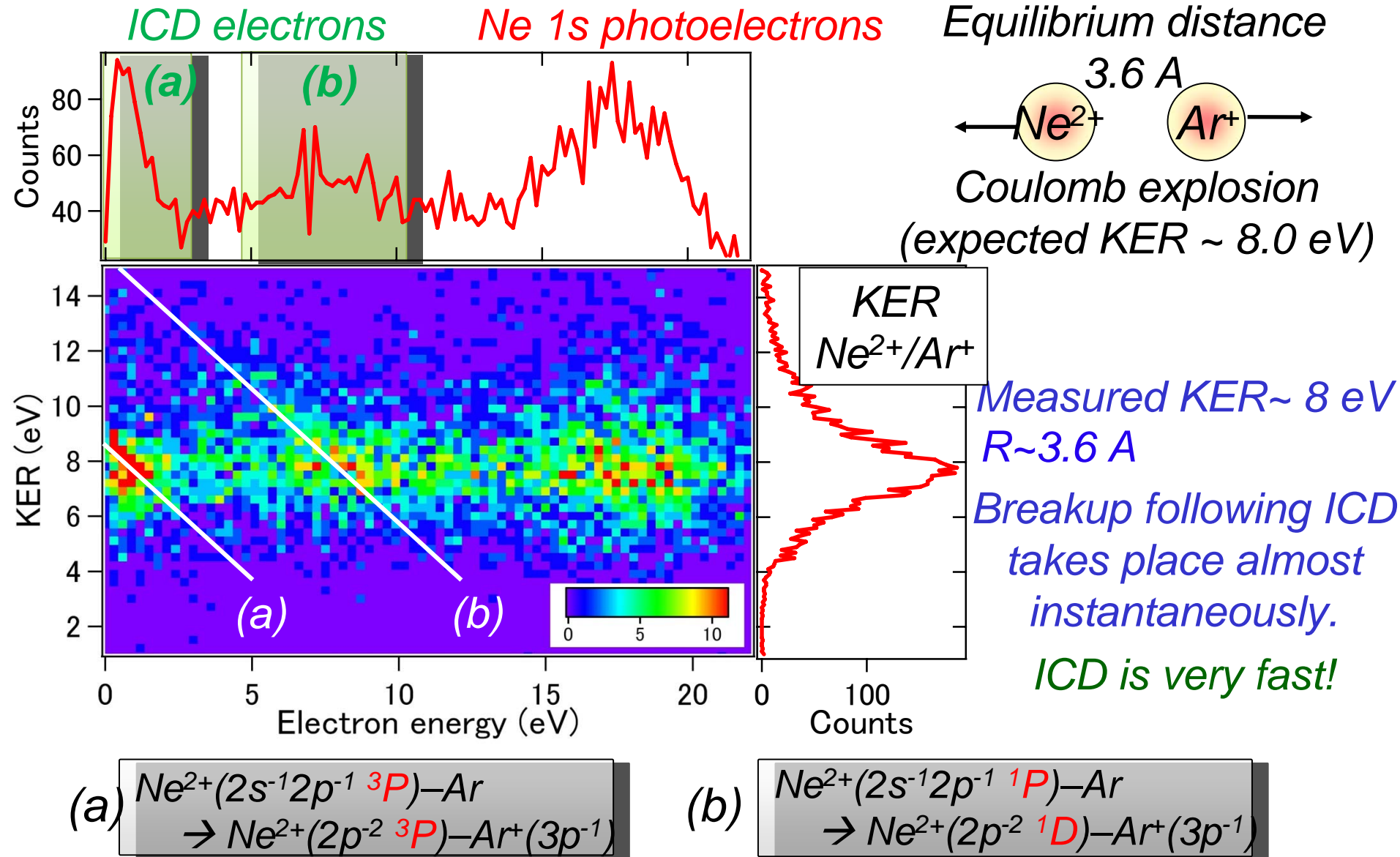
ICD in Ne-Ar after Ne 1s Auger decay



We detect ICD electrons in coincidence with Ne^{2+} and Ar^+ using e-i-i coincidence momentum imaging

ICD in Ne-Ar after Ne 1s Auger decay

Electron ion coincidence map



ICD and ETMD after triple ionization

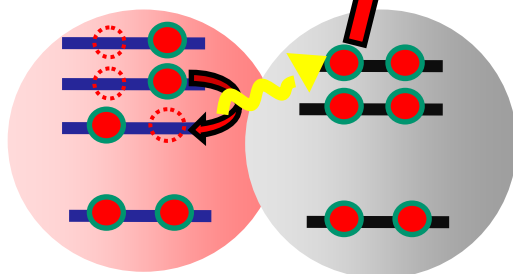
Triple ionization can occur by double Auger decay

interatomic Coulombic decay

electron-transfer-mediated decay

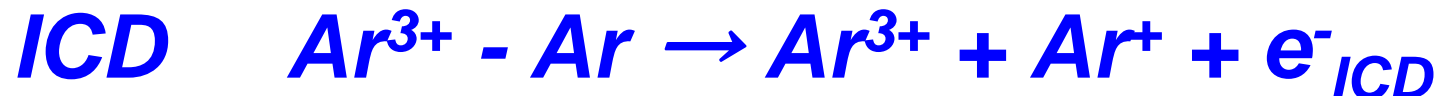
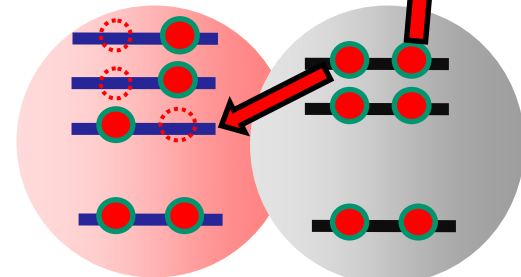
ICD

ICD electron



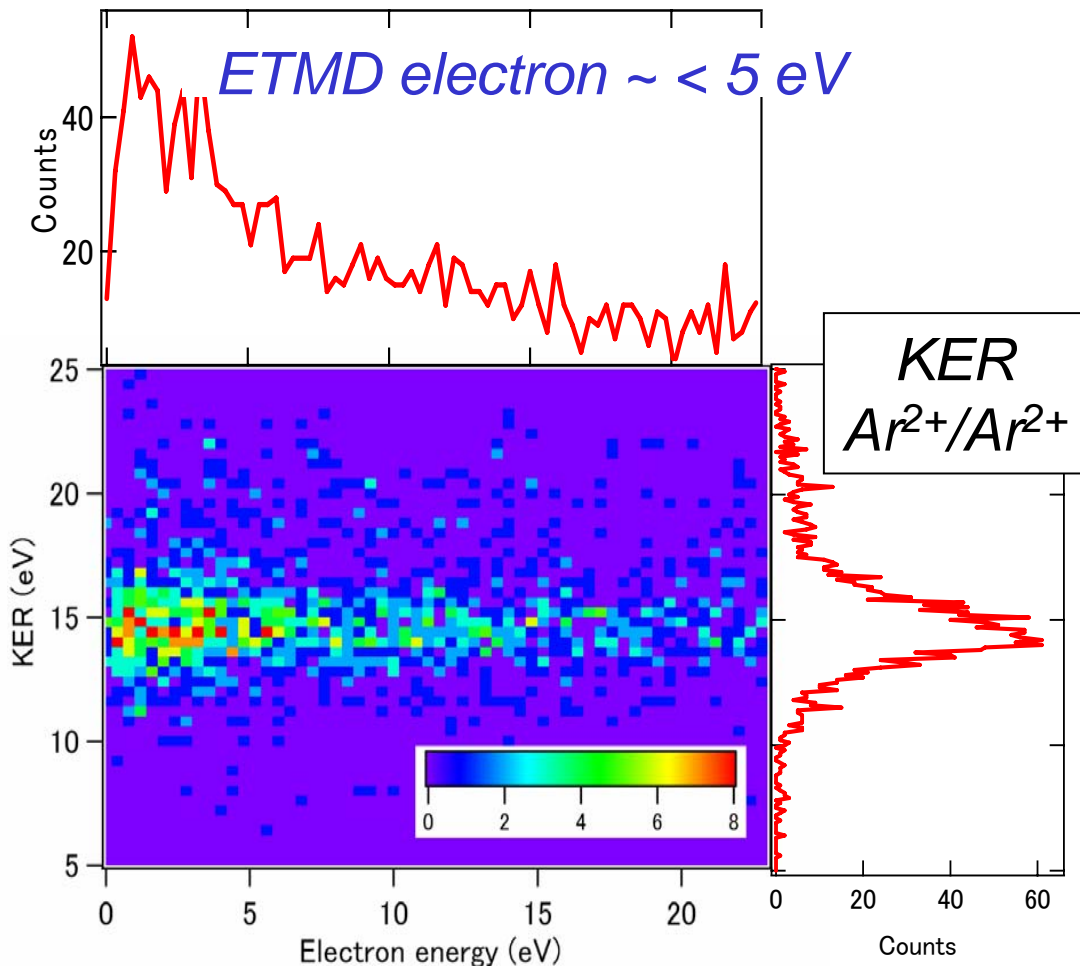
ETMD

ETMD electron

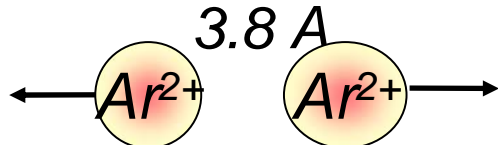


We can distinguish ETMD from ICD

ETMD in Ar₂ after triple ionization



Equilibrium distance



Coulomb explosion

(expected KER ~ 15.2 eV)

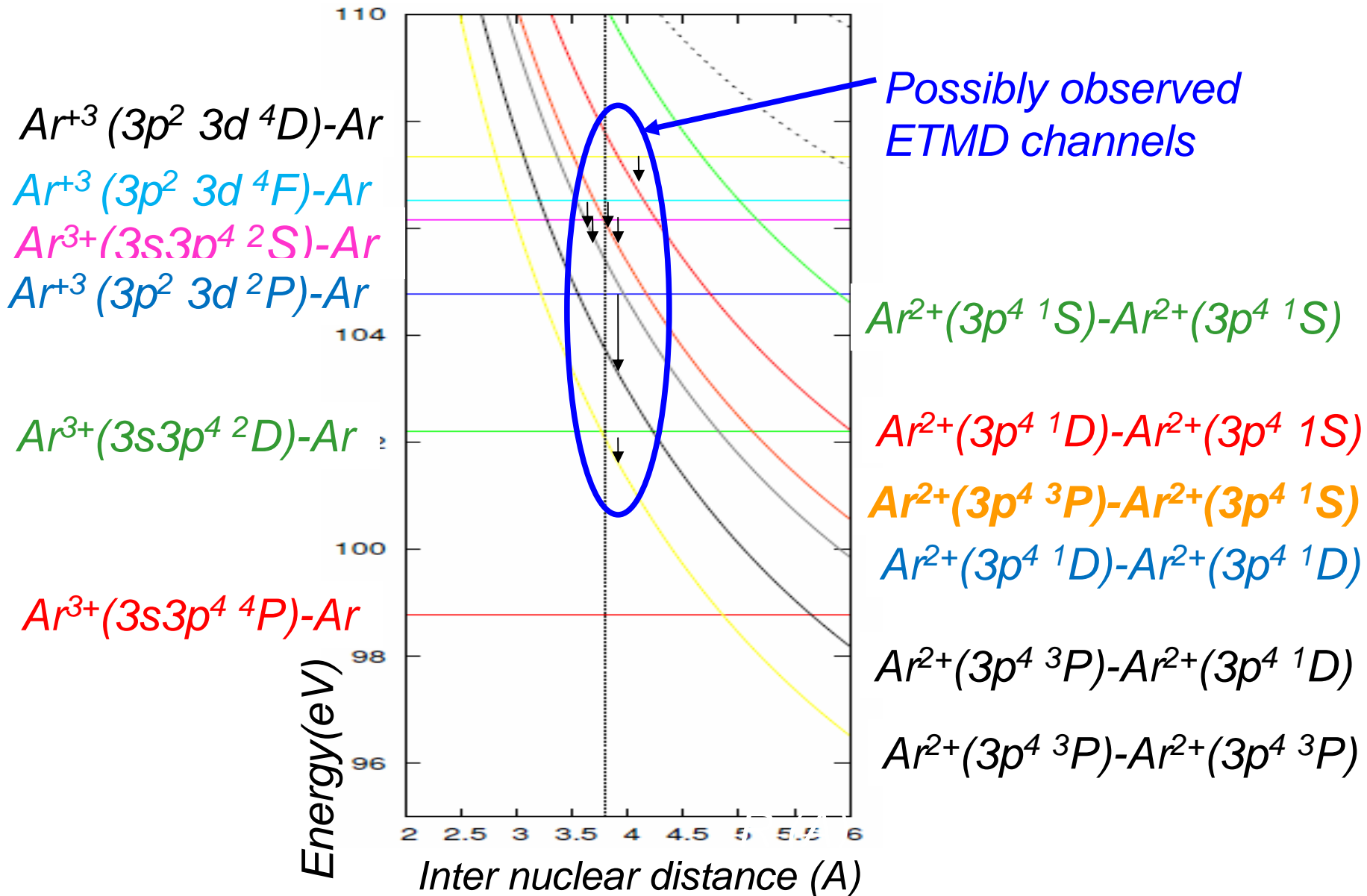
Measured KER ~ 14 eV

R = 4.1 Å

Breakup following ETMD takes place almost instantaneously.

first observation of ETMD

ETMD in Ar_2 after triple ionization



ICD collaborations at SPring-8

K. Sakai, T. Ouchi, H. Fukuzawa, T. Mazza,

K. Ueda (Tohoku U.)

I. Higuchi, Y. Tamenori (JASRI/SPring-8)

H. Iwayama, K. Nagaya, M. Yao (Kyoto U.)

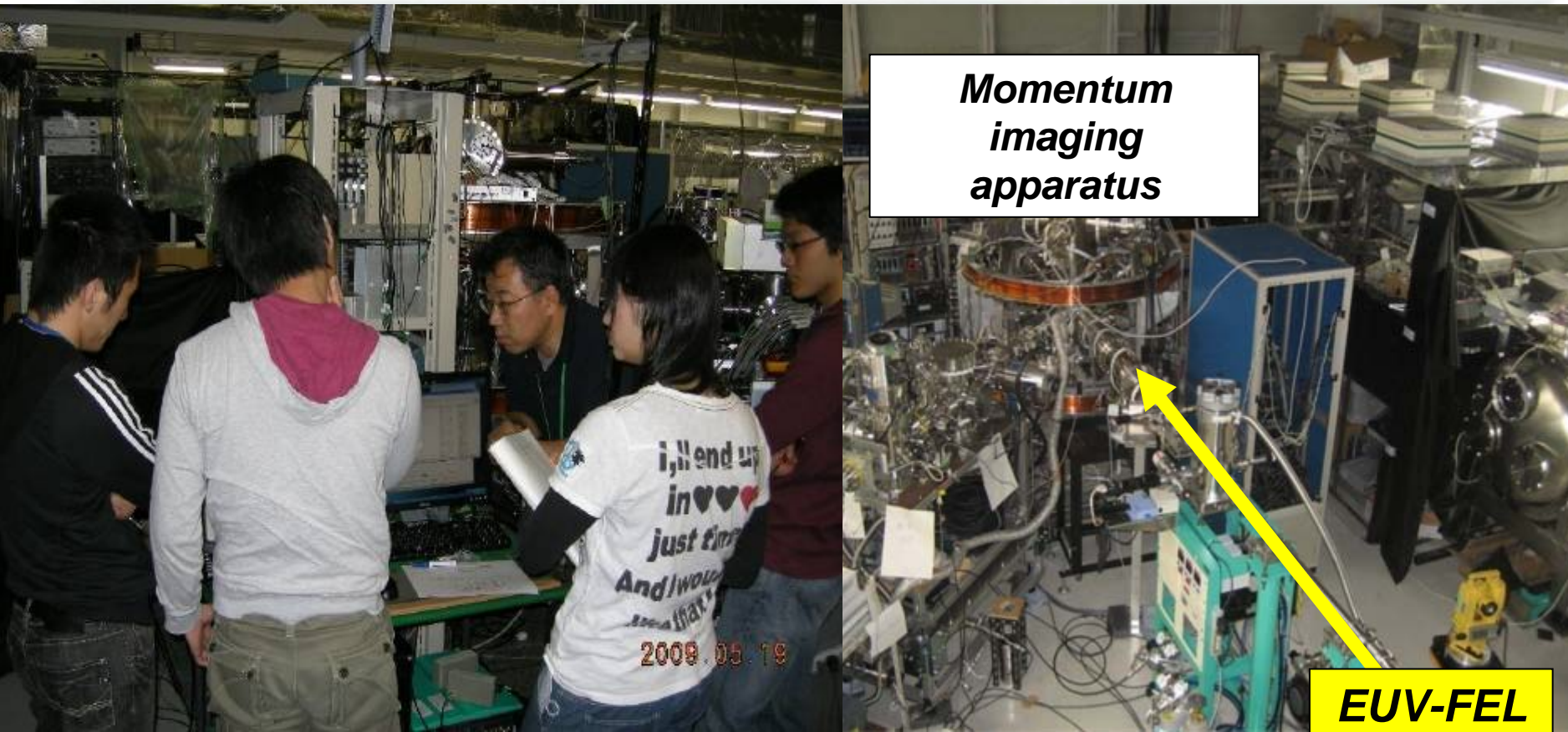
N. Saito (AIST)

D. Zhang, D. Ding (Jilin U.)

M. Schoffler (LBNL)

S.D. Stoychev, A.I. Kuleff, L.S. Cederbaum (Heidelberg U.)

SCSS test accelerator : EUV-FEL



Faciliy: EUV-FEL (SASE), RIKEN, Harima

Wavelengths : 51 ~62nm

pulse energy : $\sim 30 \mu\text{J}$ at source point

pulse duration : $\sim 30 \text{ fs}$

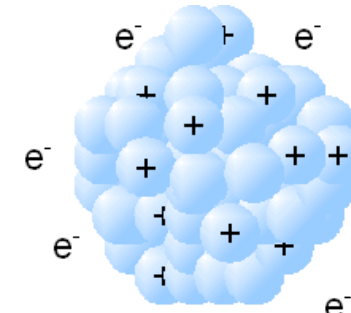
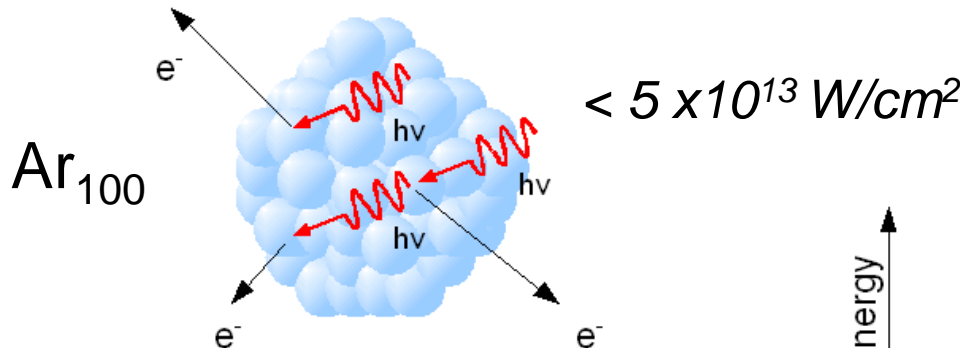
focus size : $> 3 \sim 20 \mu\text{m}$

Laser power : $\lesssim 10^{14} \text{ W/cm}^2$

Frustration of the cluster ionization

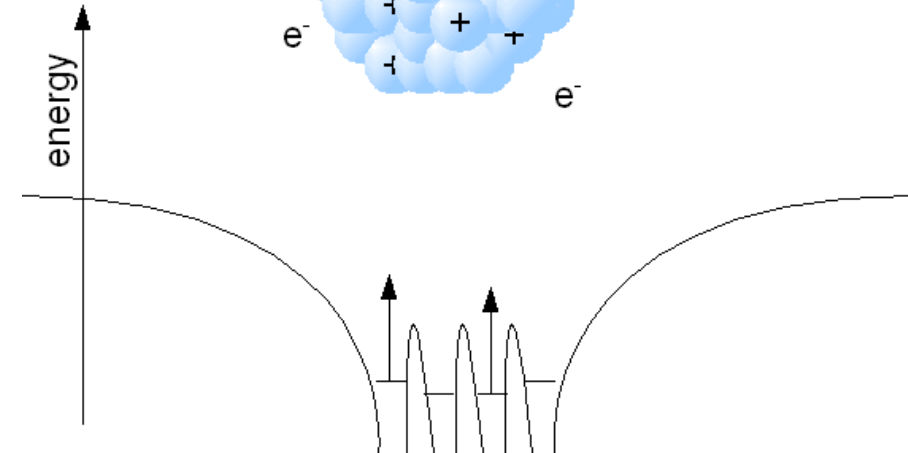
Bostedt et al., PRL 100, 133401 (2008)

Ionization energy of atomic Ar (14.6 eV) < 37.8 eV



Each individual atom will be ionized

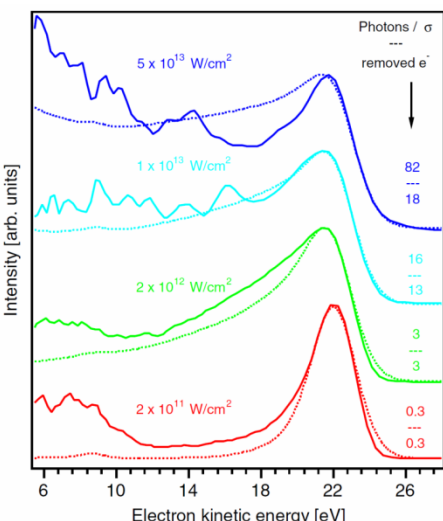
Coulomb attractive potential increases with the increase in the charge of the parent cluster.



The photoelectron cannot escape from the cluster.
Inner ionization occurs but outer ionization is prohibited.

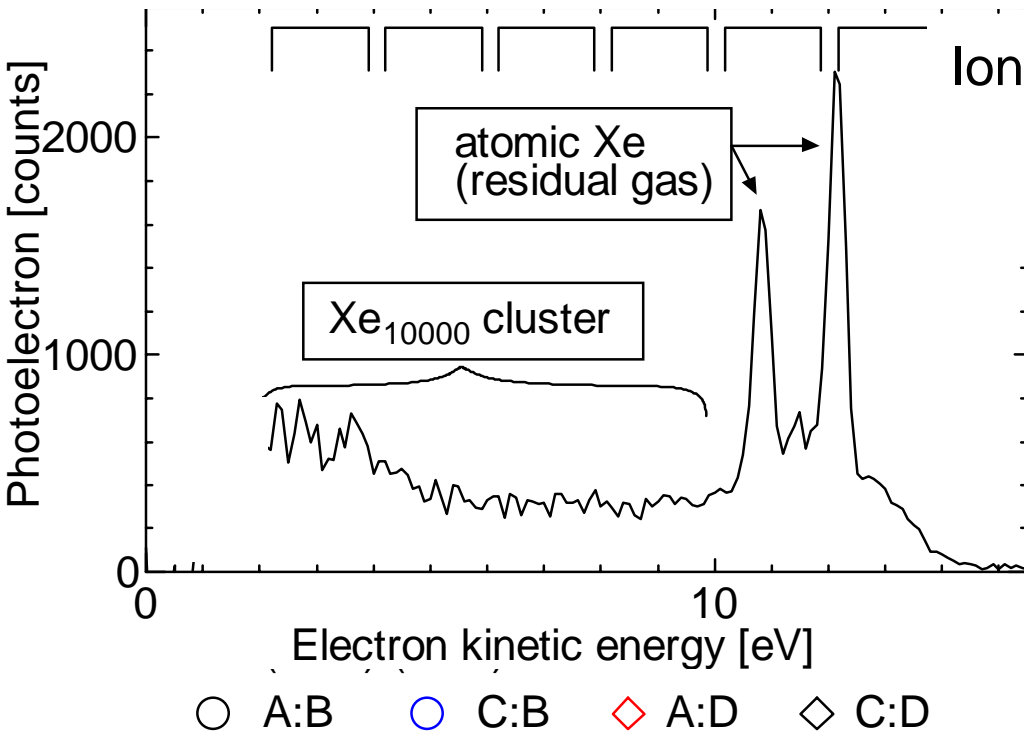
Frustration of the cluster ionization

Low energy photoelectron emission is due to lowering of the ionization potential with the increase in the charge of the cluster.



*Fukuzawa et al., PR A 79, 031201 (R) (2009);
Iwayama et al., JPB 42, 134019 (2009).*

Electron emission from the Xe_{10000} cluster

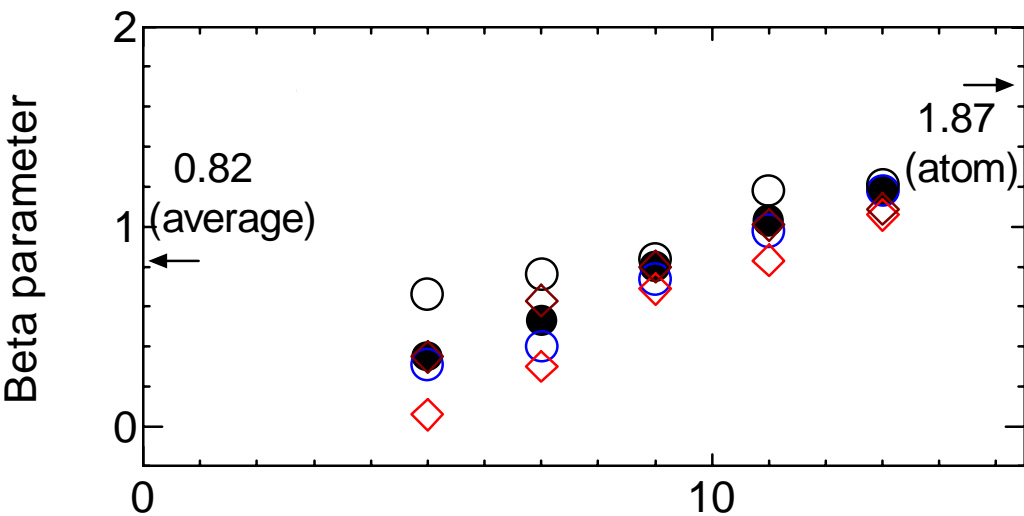


Ionization energy of atomic Xe 12.13 eV
FEL photon energy 20.3 eV
Power density $< 10^{13} \text{ W/cm}^2$

Continuous electron emission is observed as evidence of lowering of the ionization potential of the charged clusters. We evaluated the energy dependence of beta parameter.

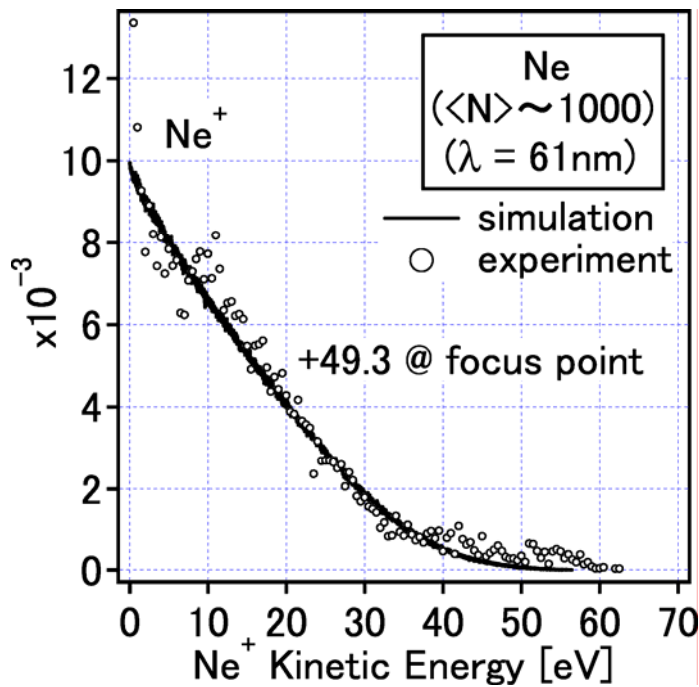
Beta value decreases with decrease in kinetic energy!

What happens with the trapped electrons?



Electronic decay of multiply excited Ne clusters ($\langle N \rangle = 1000$)

62 nm (Ne 2p->3d excitation)

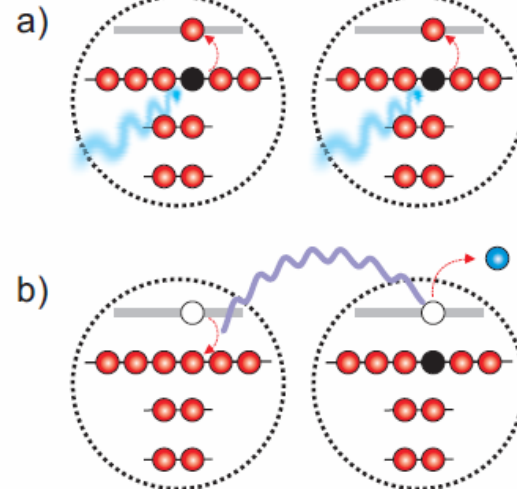
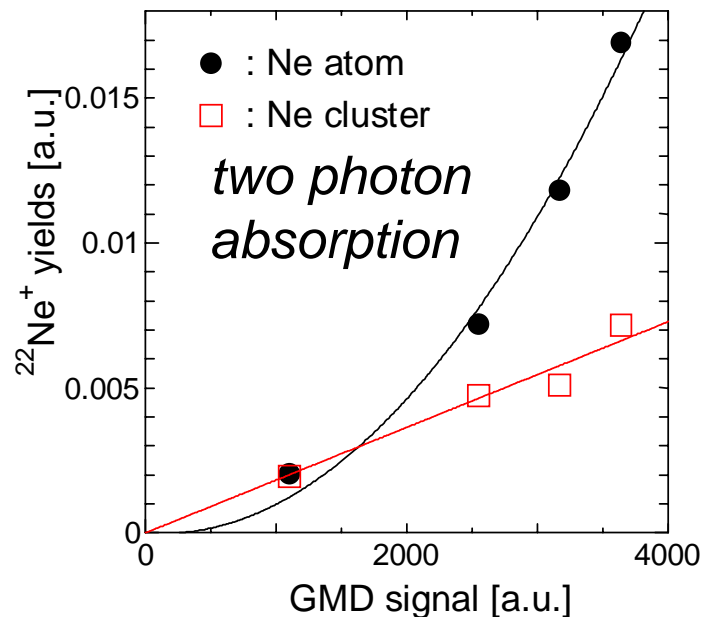


We analyzed kinetic energy distributions of energetic atomic ions using spherical uniform cluster analytical model (Islam et al PRA 73, 041201(R) 2006).

We found ~ 100 photons are absorbed and ~ 50 electrons are emitted.

How will the charge be distributed?

Nagaya et al, to be published



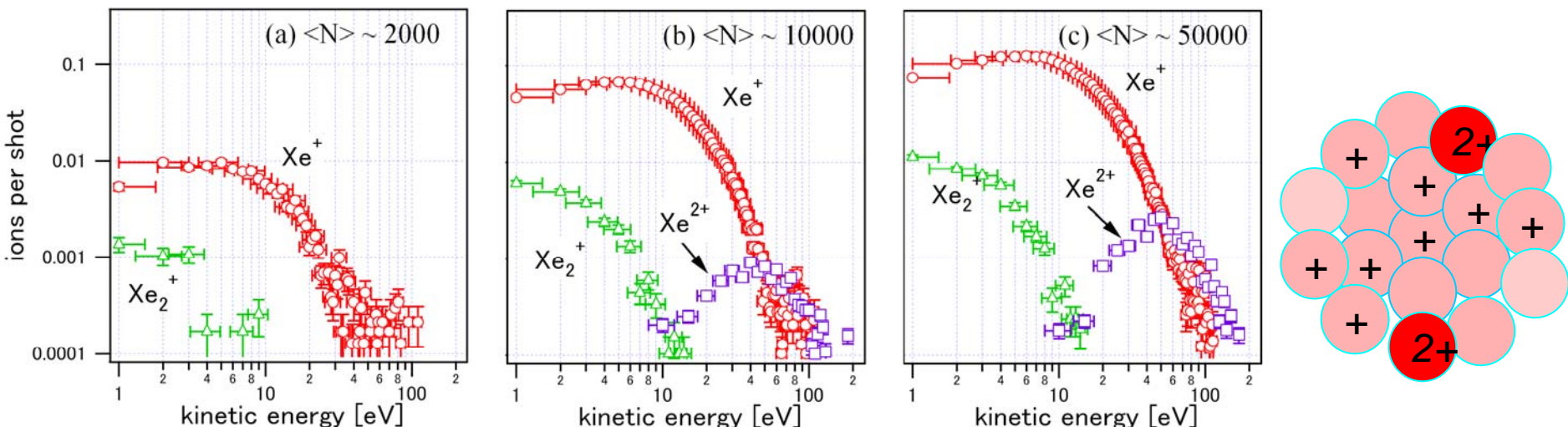
Ultrafast interatomic Coulombic decay in multiply excited clusters (Kuleff et al)
38

Xe clusters ($\langle N \rangle = 2000, 10000, 50000$) at 52nm

Kinetic Energy Distribution of the daughter ions

Kinetic Energy of Xe_2^+ : ~ 1 eV
 Xe^+ : ~ 10 eV
 Xe^{2+} : ~ 50 eV

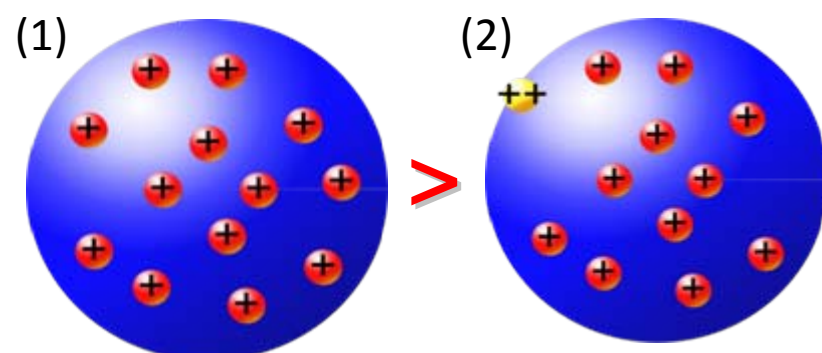
Kinetic Energy Distribution of Xe^{2+} has a hollow distribution.



The FEL power is sufficiently high to ionize the Xe atom up to +4, but for the clusters, multiply charged ions emerge only from giant clusters.



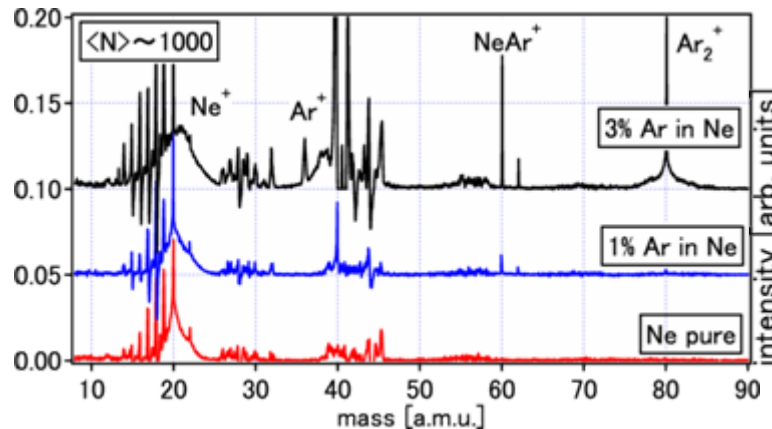
charge redistribution!



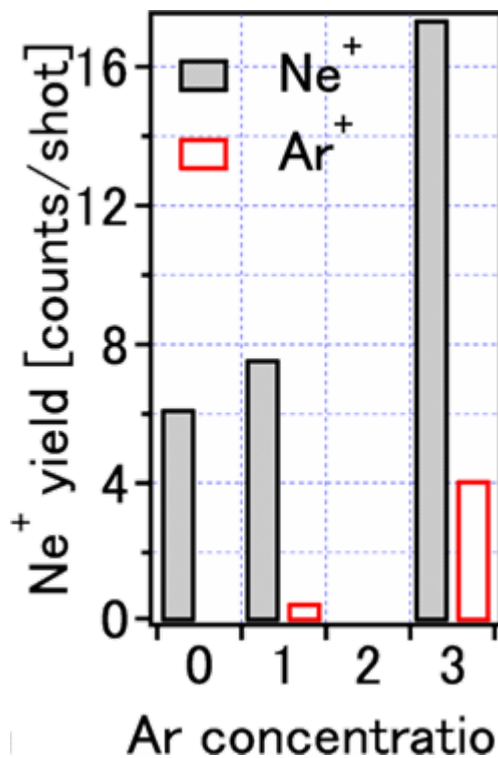
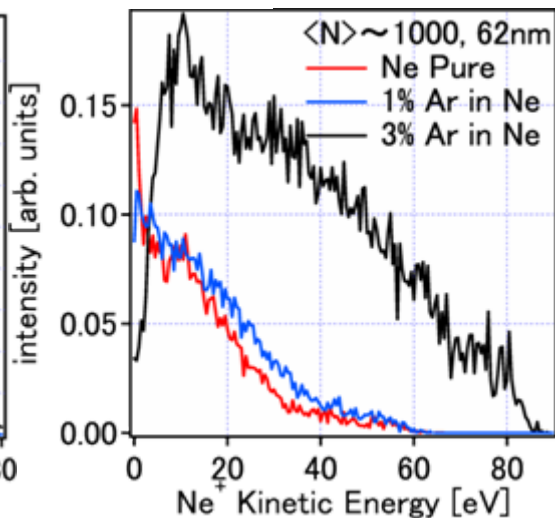
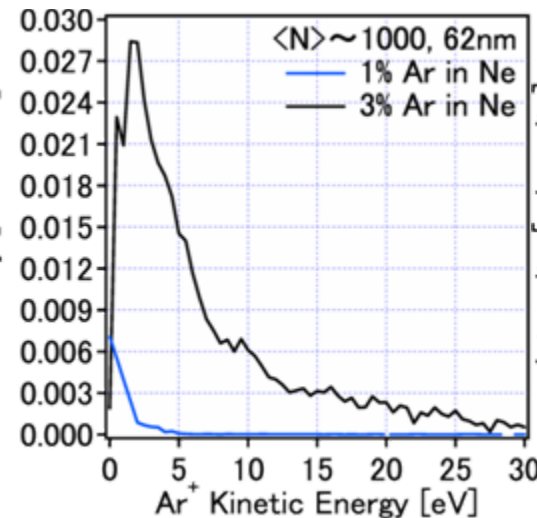
Iwayama et al., to be published.

Ar core/Ne shell clusters ($\langle N \rangle = 1000$) at 62nm

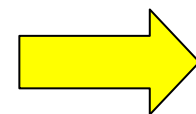
Ion TOF spectra



Ion kinetic energy distributions



The kinetic energy of Ar⁺ is much smaller than Ne⁺.



The Ar core-Ne shell structure of Ne-Ar cluster is confirmed.

With increasing Ar mixing ratio, the average kinetic energy and the yield of Ne⁺ become large.



Evidence that charges produced at the Ar core migrate to the Ne shell.

Summary of the EUVFEL Cluster experiments

We have investigated multiple ionization of rare-gas nano-clusters

We found frustration of the cluster ionization and absorption

We found interatomic Coulombic decay in multiply excited neon clusters

We found self charge redistributions to minimize the energy in highly charged argon and xenon nano-clusters

We found charge transfer from Ar-core to Ne-shell

Collaborators on EUVFEL

			ASG-CFEL, MPQ, MPI-K
<i>Tohoku U.</i>	<i>Kyoto U.</i>	<i>Frankfurt U.</i>	A. Rudenko
<i>H. Fukuzawa</i>	<i>K. Nagaya</i>	A. Czasch	L. Foucar
<i>X.J. Liu</i>	<i>H. Iwayama</i>	O. Jagutzki	O. Herrwerth
<i>K. Motomura</i>	<i>H. Murakami</i>	H. Schmidt-Boecking	M. Lezius
<i>A. Yamada</i>	<i>A. Sugishima</i>	R. Dörner	M. F. Kling
<i>G. Pruemper</i>	<i>Y. Mizoguchi</i>	<i>Detector</i>	M. Kurka
<i>M. Okunishi</i>	<i>M. Yao</i>	<i>Milan U.</i>	Y. Jiang
<i>K. Shimada</i>	<i>RG Cluster</i>	M. Devetta	K.-U. Kühnel
<i>K. Ueda</i>	<i>RIKEN, JASRI</i>	T. Mazza	R. Moshammer
<i>Apparatus, Measurements, Analysis</i>	<i>M. Nagasono</i>	P. Pizeri	J. Ullrich
<i>AIST</i>	<i>A. Higashiyama</i>	P. Milani	<i>FEL pump-FEL probe LBL</i>
<i>N. Saito</i>	<i>K. Tono</i>	<i>Metal Cluster CNR (Rome)</i>	<i>A. Belkacem Optics</i>
<i>Absolute intensity</i>	<i>M. Yabashi</i>	M. Coreno	<i>Uppsala U.</i>
<i>IMS</i>	<i>T. Ishikawa</i>	<i>Measurements</i>	R. Feifel
<i>M. Tashiro</i>	<i>H. Kimura</i>	AMOLF, Lund U.	<i>Measurements</i>
<i>M. Ehara</i>	<i>T. Togashi</i>	P. Johnsson	<i>Moscow U.</i>
<i>Hiroshima U</i>	<i>H. Ohashi</i>	A. Rouzee	E. Gryzlova
<i>O. Takahashi</i>	<i>Y. Senba</i>	M. Vrakking	<i>A. Grum-Grzhimailo</i>
<i>Theory</i>	<i>U. Tokyo</i>	<i>UV pump-FEL probe</i>	<i>Theory And More....</i>
	<i>K. Ishikawa</i>		
	<i>Theory</i>		

A wide-angle photograph of a coastal scene at sunset. The sky is filled with soft, pastel-colored clouds in shades of orange, pink, and blue. In the background, a range of mountains is visible, their peaks partially obscured by the atmosphere. The middle ground shows a calm body of water with a few small boats. On the far shore, there's some low-lying vegetation and what appears to be a small town or marina. In the foreground, a sandy beach meets the water, with gentle waves breaking onto the shore. The overall mood is peaceful and scenic.

Thank you very much for your attention!

Santa Barbara